Numerical Studies on Vacuum Consolidation in Soft Clay Deposits

Ayush Kumar

A Dissertation Submitted to
Indian Institute of Technology Hyderabad
In Partial Fulfillment of the Requirements for
The Degree of Master of Technology

भारतीय प्रौद्योगिकी संस्थान हैदराबाद
Indian Institute of Technology Hyderabad

Department of Civil Engineering

July, 2018

Declaration

I declare that this written submission represents my ideas in my own words, and where others' ideas or words have been included, I have adequately cited and referenced the original sources. I also declare that I have adhered to all principles of academic honesty and integrity and have not misrepresented or fabricated or falsified any idea/data/fact/source in my submission. I understand that any violation of the above will be a cause for disciplinary action by the Institute and can also evoke penal action from the sources that have thus not been properly cited, or from whom proper permission has not been taken when needed.
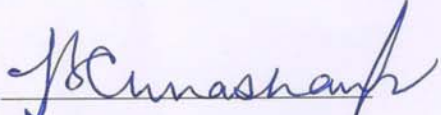
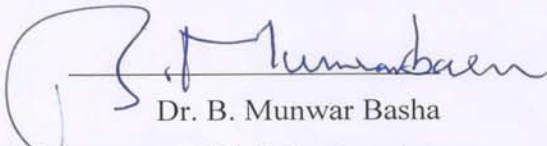(Signature)

Ayush Kumar
CE16MTECH11010

Approval Sheet

This thesis entitled "Numerical Studies on Vacuum Consolidation in Soft Clay Deposits" by Ayush Kumar is approved for the degree of Master of Technology from IIT Hyderabad.

Dr. Umashankar Balunaini
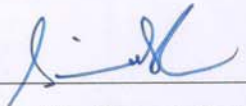Assoc. Professor, Dept. of Civil Engineering
Examiner

Dr. B. Munwar Basha
Asst. Professor, Dept. of Civil Engineering
Examiner

Dr. Sireesh Saride
Assoc. Professor, Dept. of Civil Engineering
Adviser

Dr. Suryakumar S.
Assoc. Professor, Dept. Of Mechanical Engineering
Chairman

Acknowledgements

Dedicated to

My family who stood by me thick and thin

Abstract

Vacuum consolidation is a promising technic to accelerate the consolidation process of soft soils under favorable conditions over other processes. It is essential to stabilize these soils to improve load carrying capacity and reduce the consolidation behaviour. Vacuum consolidation method reduces the pore water pressure inside the soil mass without the requirement of any additional fill loading, thus eliminating the possibility of shear failure, allowing faster and safer construction.

In this study, coupled flow deformation analysis is adopted to perform a numerical analysis of vacuum consolidation in soft clay deposits. A numerical model is formulated using PLAXIS 2D, a finite element software. Soft soil model is used to model the behaviour of soft marine clay. PVDs are modelled using linear drain elements under negative vacuum pressure. The model is simulated in the study of clay deposits at Kakinada port, India. The geotechnical data was adopted from the case study available in the literature. The numerical simulations confirmed that there was a vacuum loss in the field. The magnitude of available vacuum pressure in the field was predicted by several numerical simulations. Mandel-Cryer effect was observed initially because of application of vacuum pressure between the PVDs. Influence of staged vacuum application during initial period is also studied. With the numerical study 85-90% reduction in post-construction settlements were observed.

Equation of radial consolidation is solved using the finite difference method with a wide range values of coefficient of radial consolidation (C_r) and drain spacing ratio (n). The solutions obtained are presented in form of a design chart to obtain the desired degree of consolidation (U) with respect to radial time factor (T_r). The chart is validated with the available case studies in literature. The results were found to be in good agreement with the published data for homogenous soil strata.

Nomenclature

σ	total stress
σ'	effective stress
u	pore water pressure
U	Degree of consolidation
U_{avg}	Average degree of consolidation
T_r	Radial time factor
C_r	Coefficient of radial consolidation
PVD	Prefabricated vertical drain
d_w/r_w	equivalent/radius drain diameter
d_e/r_e	diameter/radius of influence of a PVD
d_s/r_s	diameter/radius of smear zone
u_s	suction pressure
u_0	initial pore pressure
ξ	local coordinate for triangular element
η	local coordinate for triangular element
ζ	auxiliary coordinate for triangular element
N_i	shape function at i^{th} node of the triangular element
$\lambda*$	modified compression index
$\kappa*$	modified swelling index
M	slope of the critical state line
VP	vacuum pressure
CSL	critical state line
I_e	target element size
r_e'	relative element size factor

Contents

List of Figures

List of Tables

Chapter 1

Introduction

1.1 Preamble

Ground Improvement techniques have been increasingly used to stabilize the weak soils and improve their geotechnical properties like shear strength, compressibility and permeability. With the increase in population, more land is needed for infrastructure facilities like ports and industries. Thus, many coastal regions are witnessing land reclamation projects. These coastal areas often have very thick deposits of soft soil which are in equilibrium with their own self weight and a small increase in external load may cause a large settlement and instability.

Foundations like pile foundations in these soils may prove to be ineffective because of the large depth of deposits. Soil improvement is considered to be a better option in such cases. Different methods like surcharge preloading, sand drains, stone columns, wick drains and deep soil mixing have been successfully used in several large scale projects. Each site may require a different method of treatment, based upon the strata, accessibility and availability of resources. The major factors to be considered are importance of the facility coming up, time available for the ground treatment and economics involved which will affect the procurement of specialized equipment and workforce. Following sections briefly discuss about the different ground improvement technics adopted in such cases.

1.2 Preloading

Preloading results in reduction of water content of the soil, thus increasing its shear strength and lessen post construction settlements. In order to accelerate the consolidation process, vertical drains are used in conjunction with surcharge or vacuum preloading. Vertical drains provide a much shorter drainage path in horizontal direction for dissipation of excess pore pressure, thus reducing the consolidation time drastically.

Surcharge Preloading

Surcharge preloading involves construction of a soil embankment over the treatment area. Excess pore pressure is generated in clay because of their low permeability. As the excess pore pressure slowly dissipates, the soil mass gets squeezed, resulting in settlement at surface. Besides, building a surcharge preload requires heavy machinery and the work needs to be executed slowly else the excess pore pressure generated will cause bearing capacity failure. Hence, surcharge preloading alone is an obsolete technic, unless the construction sites are idle for a long time. Detailed design methods are available to implement the technic.

Vacuum Preloading

In the recent decades, the use of atmospheric loading system, i.e. *vacuum consolidation* has become popular and widely adopted in coastal regions for improving very soft clay and peaty soils. Vacuum pressure is applied using a vacuum pump and is transferred to the soil with the help of prefabricated vertical drains (PVDs). The increase in the effective stress in the soil is equal to the vacuum pressure (negative excess pore pressure) applied. It is possible to achieve up to 80-85 kPa of effective vacuum pressure in the field, thus reducing the need for surcharge load. The rate of consolidation in vacuum consolidation and equivalent surcharge preloading is same [1]. However, vacuum preloading offers several advantages over conventional surcharge preloading technique such as there is no requirement of fill material, no possibility of shear failure and shorter construction period. Figure 1.1 shows treatment of ground using vacuum consolidation method.

Figure 1.1: Vacuum preloading along with PVDs (Image courtesy: COFRA)

Nowadays surcharge and vacuum preloading are used together in order to check the lateral movement. The excess pore pressure generated by the surcharge is dissipated by the negative (vacuum) pressure applied by the vacuum pump. In addition, vacuum preload being isotropic in nature, induces inward movement of soil. While, the surcharge load causes outward movement of soil mass. Thus a balance between the two techniques allows one to keep the lateral movement under check. Figure 1.2 shows the comparison of lateral displacements observed in surcharge and vacuum preloading techniques [2].
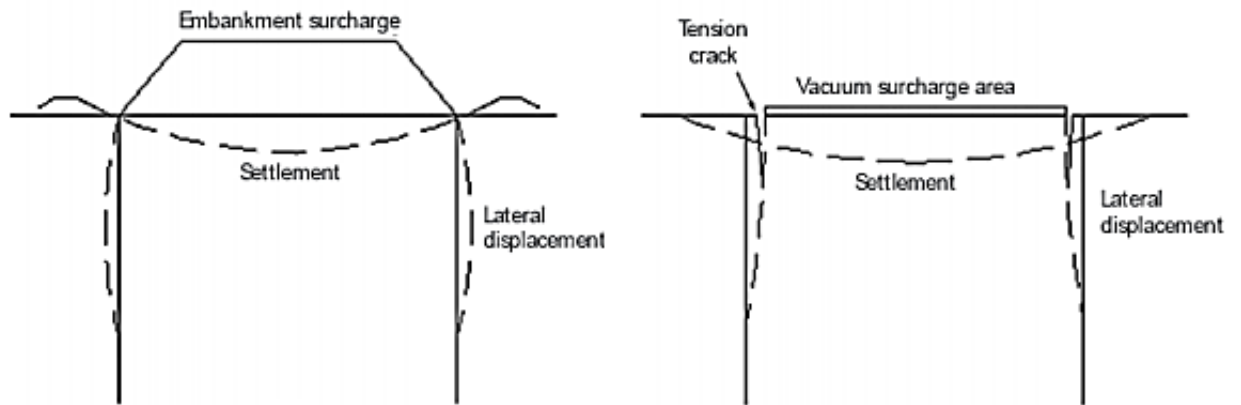
Figure 1.2: Comparison of lateral deformation in soil due to surcharge and vacuum preload [2]

1.3 Vacuum Consolidation System and Construction

Primary application of vacuum consolidation system is stabilization of soft clayey soil by achieving required degree of consolidation in pre-construction phase. Principally, the system consists of system of vertical drains connected to horizontal drains as part of surface drainage at the top to carry the discharged water away from the treatment area. Airtight membrane is used to isolate the treatment area from the surface. Figure 1.3 shows a schematic of Vacuum Preloading system developed by Menard Group. The important components in the vacuum preloading are vertical drains, surface drains and impermeable membrane.
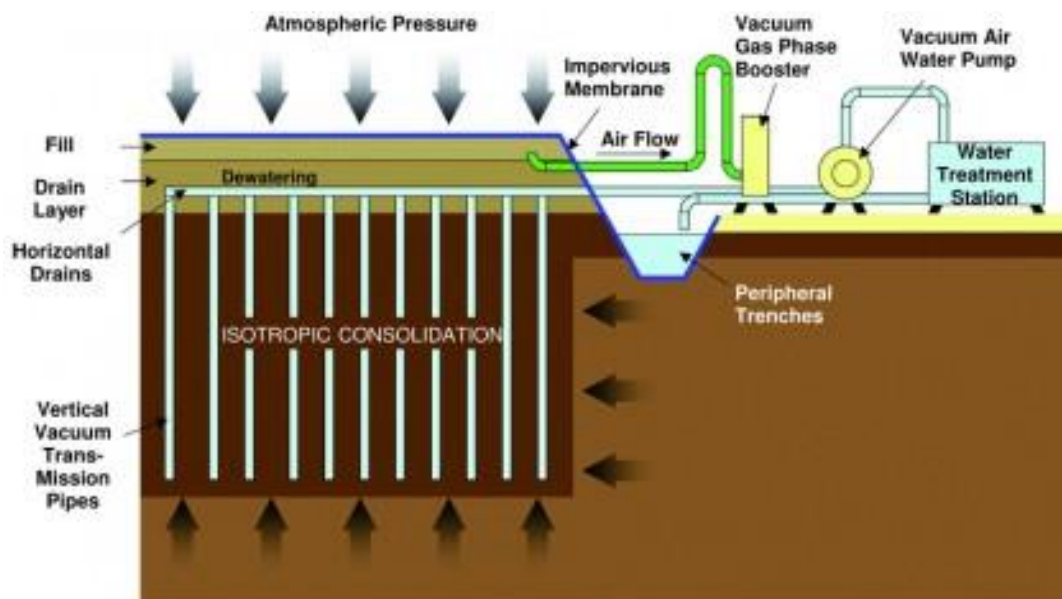
Figure 1.3: Menard Vacuum Preloading system (*Image courtesy: VIBROMENARD*)

Vertical Drains

Vertical drains are an important part of the vacuum consolidation system as these are the medium to transfer vacuum pressure to the treatment area. Different vertical drains have been developed across the world, but the most common type of vertical drain used is the PVDs. These are highly permeable drains, can be installed easily with a minimal disturbance to the soil deposit and at high speed and have been proven to be cost effective. However, these drains have some environmental impact as well because of their non-biodegradable nature, nevertheless, the PVDs continue to act as drainage paths for future and for unexpected higher loads.

Surface drainage

Surface drain is normally a granular layer of sand and a network of horizontal collector pipes which connect to the main vacuum pipe. This sand layer is generally 0.3 m to 0.5 m thick, however if the thickness needed, can be increased to serve as a working platform.

Impermeable Membrane

The system also needs to be properly isolated (sealed) from the surroundings for attaining a desired vacuum pressure and hence the required degree of consolidation. Mostly, this is achieved by covering the entire area with an airtight membrane. Also, the membrane edges are keyed in peripheral trenches excavated to a depth at least 0.5 m below the groundwater

table and filled with impervious slurry (generally Bentonite). Another technique is from Menard system, in which a 1.5m thick primary fill is constructed directly on the top of the sand mat beneath the membrane for increasing the stability and sealing of the system. This fill will retain the soil just below the membrane in non-submerged condition [3].

1.4 Mechanism of Vacuum Preloading

The mechanism for vacuum consolidation can be explained by the spring analogy (Figure 1.4b) described by Chu and Yan (2005) [4]. When the vacuum pressure is applied, the pore pressure in the soil mass reduces. Now, since the total stress remains constant, the effective stress increases. The spring gets compressed gradually indicating that the soil skeleton starts gaining effective stress. Eventually, the effective stress equals the vacuum pressure applied. The effective stress during vacuum consolidation increases isotropically, i.e. the corresponding lateral stress is compressive.

This isotropic compression leads to development of surface tension cracks at the peripheries of the treatment area (Figure 1.2). However, these tension cracks are confined in a few meters from the treatment area, while the lateral displacement can be observed up to a distance of 2 to 3 times the drain depth. However, as discussed in section 1.2.2, application of surcharge load along with the vacuum preload helps control the tension cracks by balancing the inward and outward movement of soil.

$$u_0 = p_a$$
$$\Delta \sigma = p_a + \Delta p - (u_0 + \Delta u) = \Delta p - \Delta u$$

(a) Surcharge

$$u_0 = p_a$$
$$\Delta \sigma = p_a - (u_0 - \Delta u) = \Delta u$$

(b) vacuum consolidation
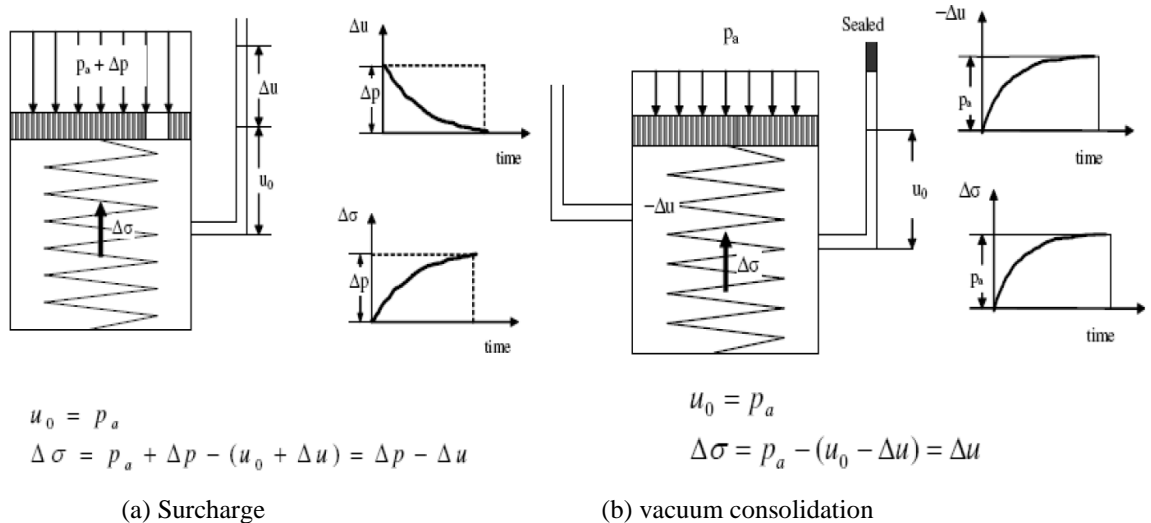
Figure 1.4: The spring analogy of (a) surcharge, (b) vacuum consolidation [5]

1.5 Modelling of Vacuum Preloading

The Numerical modelling of vacuum consolidation is challenging because it involves generation of negative excess pore water pressure along the prefabricated vertical drains.

5

Presence of smear zone, well resistance and anisotropy of soil also makes the process complicated. Performing 3D computations may be very complex and time consuming. Thus 2D analysis is considered in this study. Earlier, Rujikiatkamjorn et al. (2008) [6] established that an equivalent plane strain analysis is sufficient from a computational point of view, in case of multi-drain analysis and large infrastructure projects.

1.6 Objective and Scope of the Study

The major objective of the present study is to model the vacuum preloading technique coupled with PVDs and to develop an understanding of the influence of vacuum pressure on the consolidation behavior of soft soils using PLAXIS 2D finite element program. The scope of the present research is:

1) Development of a numerical model for vacuum consolidation
2) To understand the behavior of soft soil after vacuum consolidation
3) To develop a design chart which would help determine optimum time required to achieve desired degree of consolidation for a given vacuum pressure.

1.7 Organization of the Thesis

In **Chapter 2** the literature survey about the experimental and numerical studies on vacuum preloading method has been discussed. Discussion has been carried on modelling of drains, equivalent permeability in plane strain conditions and numerical and analytical modelling of vacuum assisted consolidation with PVDs. **Chapter 3** deals with modeling of vacuum preloading using prefabricated vertical drains. The vacuum preloading is modelled by a reduction of the groundwater head from the phreatic level in the linear drain elements. Material models used and finite element formulation are presented. The challenges and the requirements to simulate the vacuum pressure in the soil mass using PLAXIS 2D is discussed. The validation of the model using a previous study on Vietnam Port reclamation project is also discussed in this chapter. **Chapter 4** discusses the case study of Vacuum consolidation trial at Kakinada Sea Port. Results obtained using numerical simulations are compared with the previously available field observations. Influence of varying vacuum pressure on pore pressure and lateral displacement is discussed. Effect of applying vacuum pressure in stages instead of single stage is also discussed. In **Chapter 4** the various parametric studies have also been carried out to develop an understanding of the various factors which affect the degree of consolidation and outcomes of the method like time of application of surcharge along with the vacuum pressure, influence of Poisson's ratio and

6

improvement in settlement characteristics after vacuum preloading. **Chapter 5** discusses the design charts which are developed using theoretical models based on finite difference (FD) formulation to estimate the degree of consolidation (U) with respect to time factor (T_r) for various coefficient of consolidation in radial direction (C_r) and effective diameter ratio (n). The FD models were validated with the field data. A unique design chart was developed to ascertain the degree of consolidation when vacuum preloading was adopted for any type of soft soil condition. **Chapter 6** summarizes the results obtained from the study and the major conclusions drawn from the study.

Chapter 2

Literature Review

2.1 Introduction

Preloading coupled with Prefabricated Vertical Drains (PVDs), is a popular ground improvement technique for stabilization of soft clay and peat deposits and reclaimed marshy lands. Several studies are available which deal with performance of PVDs under vacuum pressure, settlements, pore water pressure changes, horizontal displacements and other aspects. In this chapter, a detailed review of the literature including numerical modelling and case studies related to vacuum consolidation is presented.

2.2 Vertical Drains

Vertical drains help in accelerating the consolidation process by shortening the drainage path. The coefficient of horizontal permeability in clay is generally higher than that of the vertical permeability because of anisotropic nature of natural clays. Thus, providing a horizontal drainage path is the best suited solution. These drains can be arranged in either triangular or rectangular pattern. Figure 2.1 shows the cross-section of a vertical drain unit cell.

Barron's theory [7] presented the solution for radial consolidation by drain wells. The solution was broadly categorized into two types:

i. *Free strain*: When the surcharge applied at the ground surface is flexible in nature, the surface load distributes equally over the ground. The settlements caused are uneven.

ii. *Equal strain*: The surcharge applied is rigid, resulting in equal settlement over the area. However, the stress distribution is unequal.
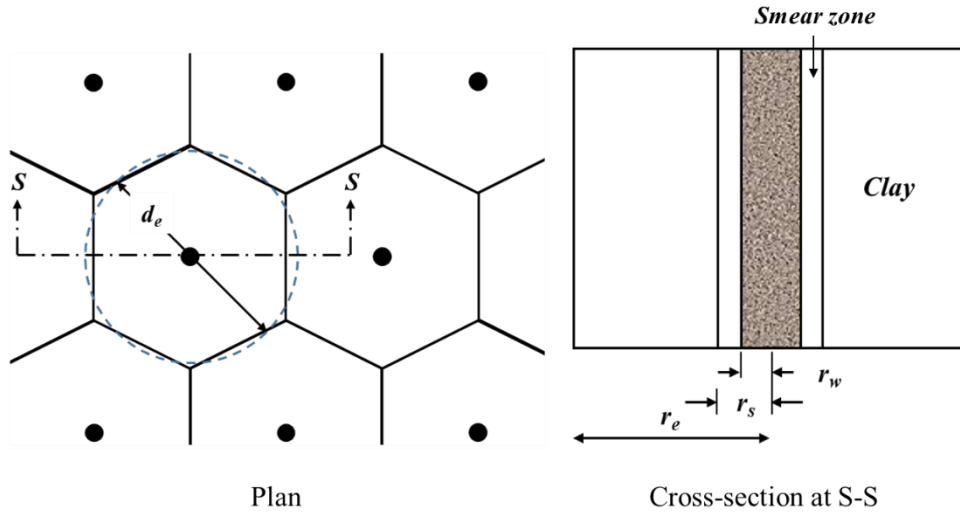
Figure 2.1: Triangular layout of vertical drains

The governing equation for dissipation of excess pore water pressure $u(t,r)$ is given by

$$\frac{\partial u}{\partial t} = C_r\left(\frac{\partial^2 u}{\partial r^2} + \frac{1}{r}\frac{\partial u}{\partial r}\right) \tag{2.1}$$

Where, u = excess pore water pressure, r = radial distance from center line of the drain and C_r=coefficient of radial consolidation

The solution of the above equation for condition of equal vertical strain without smear is given as [7],

$$U = 1 - \exp\left[\frac{8T_r}{F(n)}\right] \tag{2.2}$$

Where,

$$F(n) = \frac{n^2}{(n^2-1)}\ln(n) - \frac{(3n^2-1)}{4n^2} \tag{2.3}$$

Here n is the drain spacing ratio and is defined as $n = \dfrac{\text{Diameter of Influence } (d_e)}{\text{Diameter of drain } (d_w)}$

And, T_r = Time factor for radial flow given by $T_r = C_r\dfrac{t}{d_e^{\,2}}$ $\tag{2.4}$

9

Numerically, free strain and equal strain solution give similar results. Hence, equal strain solution is often used because of its simplicity.

Factors Affecting Drain Performance

Most common type of vertical drain used nowadays are band shaped prefabricated vertical drains (PVDs), generally of dimension 100 mm x 4 mm. They have a core in the form of longitudinal channel surrounded by a synthetic filter material cover. Chai and Miura (1999) [8] conducted studies on various factors which affect the performance and efficiency of PVDs which are presented below.
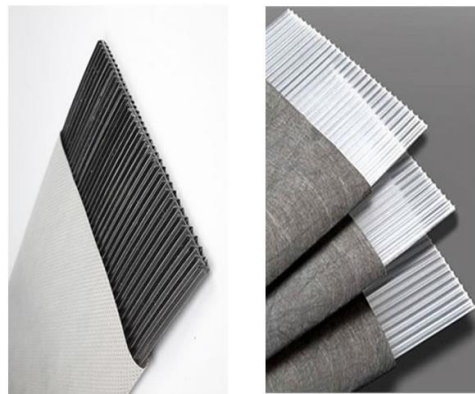
Figure 2.2: Prefabricated Vertical Drains (PVDs) (*Image Courtesy: GEOMAT INDONESIA*)

Equivalent Drain Diameter (d_w)

The solutions for vertical drains in literature [7] assume the drain to be circular in cross-section. Thus, it is important to convert the geometry of PVD to that of a circle. Hansbo (1981) [9] presented equivalent drain diameter by equating the circumference of both shapes, based on Kjellman's [10] considerations, stating that the draining effects is essentially a function of circumference of the drain and not the cross-sectional area.

The equivalent drain diameter (Hansbo, 1981) [9]

$$d_w = \frac{a+b}{\pi} \tag{2.5}$$

Where *a* and *b* are the width and thickness of the rain, respectively.

Diameter of influence (d_e)

Diameter of influence is the function of spacing of drains as well as pattern of arrangement of PVDs. For square pattern, $d_e = 1.13s$ and for triangular pattern $d_e = 1.05s$, where s is the spacing between two adjacent drains.

Smear zone

Smear zone around a PVD is the zone of reduced permeability formed because of remolding of clay during the installation by mandrel. The reduced permeability leads to decrease in overall coefficient of consolidation. Indraratna and Redana (1998) [11] suggested the extent of smear zone to be about 3-4 times the cross-sectional area of the mandrel. Sathananthan et al. (2008) [12] concluded that smear zone is 2.5 time the mandrel radius and coefficient of horizontal permeability decreased by 61-92% in smear zone.

Well Resistance

Well resistance is the resistance to flow of water into the drain. Well resistance increases with the increase in length of the drain. Well resistance increases if there is any deterioration of the filter, or if the drain gets folded due to settlement. Formation of biofilm by entry of oil particles in PVDs may cause clogging and hence, increase in well resistance. Hansbo (1981) [9] presented an analytical solution incorporating well resistance effects.

Effect of Sand Mattress

Chai and Miura (1999) [8] discussed the effect of Sand Mat on the performance of PVDs. It is generally assumed that the sand mat/blanket provided over the PVD arrangement does not offer any resistance to the outflow of water. However, in some cases, due to the scarcity of material as well as economic considerations, lower quality sand such as clayey sand is used for the sand mat. In such case, the lower permeability of the sand mat may influence the rate of consolidation.

2.3 Vacuum Consolidation

Vacuum preloading technique was first introduced by Kjellman (1952) [8]. Royal Swedish Geotechnical Institute worked out initially on this method for fine grain soil improvement. Since then, the method has gained immense popularity because of its advantages over conventional surcharge preloading. With the development of technology and manufacture of high quality drains, pumps and airtight sheets, the method overcame the initial hurdles like maintenance of effective vacuum pressure in the ground. Over time, the vacuum preloading technique has been successfully employed for ground improvement projects for

infrastructure like ports, highways, airport runways, industries etc. in China, USA, Japan, and South East Asia predominantly.

2.4 Experimental Studies on Vacuum Preloading

Mechanism of vacuum consolidation and determination of degree of consolidation, deformations have been reported in literature ([8], [10], [13-15]). A brief review of the information available in literature about various experimental studies is discussed below.

Mohamedelhasan and Shang (2002) [16], after studying a combined vacuum and surcharge model, concluded that properties obtained from 1-D consolidation tests can be used for design problems involving vacuum preloading. Later, Indraratna et al. (2004) [13] conducted large scale laboratory testing using vacuum pressure of 100 kPa. It was noticed that the occurrence of soil unsaturation at the PVD boundary could retard the pore water pressure dissipation. The study emphasized on need to have correct soil moisture characteristic curves.

Chai et al. (2005) [15], proposed an approximate method to calculate ground settlement and inward lateral deformation. Laboratory studies suggested that vacuum pressure larger than the lateral stress required to maintain K_0 condition, which will lead to an inward lateral deformation. The theory was verified using field data available from two case histories in China. A soil element deformation pattern with and without considering lateral deformation is shown in Figure 2.3.
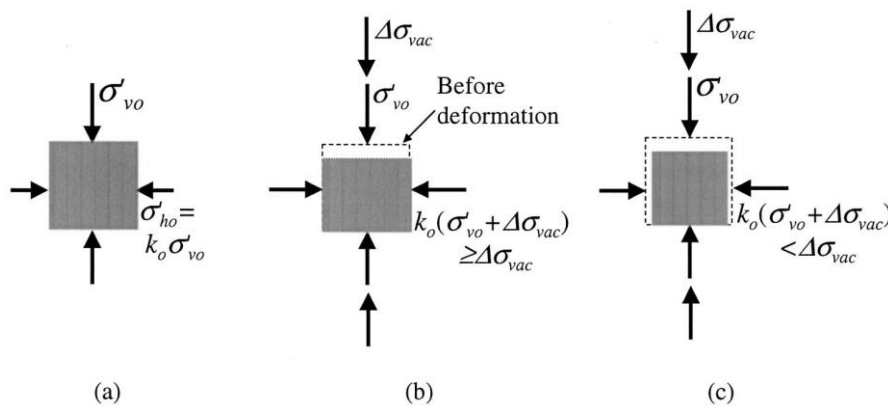
Figure 2.3: Soil element deformation pattern; (a) initial stress state; (b) no lateral displacement; and (c) with lateral displacement [15]

Robinson et al. (2012) [14], performed a study using modified Rowe cell apparatus for allowing lateral deformations to occur. It was concluded that the change in volume of soil is isotropic (Fig. 2.4). The study introduced the existence of three stress states in soil at different depths, namely, tension zone, active zone and at-rest zone.
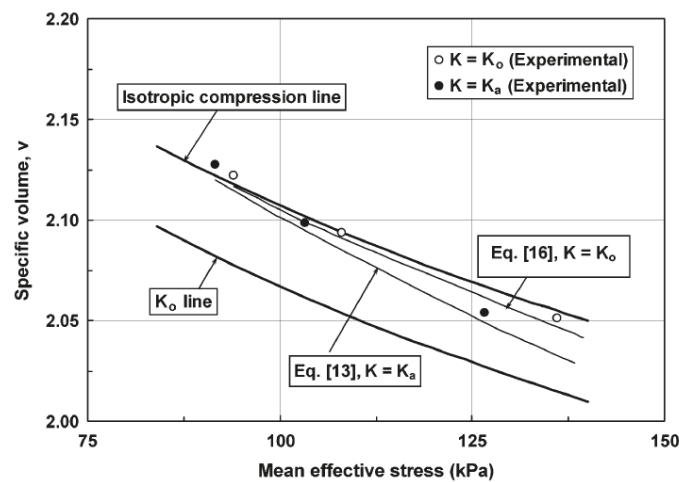
Figure 2.4: Predicted and measured values of specific volume for different vertical effective stress values. K, coefficient of earth pressure (Robinson et al., 2012)

Gangaputhiran et al. (2016) [17] compared the behavior of soil after surcharge and vacuum preloading. From laboratory investigations, it was observed that vacuum preloaded samples showed less anisotropy in permeability than surcharge preloaded samples. Scanning Electron Microscope (SEM) images have shown that at shallow depths, vacuum preloaded samples displayed more flocculated structures while surcharge preloaded samples showed dispersed arrangement.

2.5 Numerical Studies on Vacuum Preloading

The soil shows complex behavior under vacuum or surcharge preloading with vertical drains. Several finite element (FE) and finite difference (FD) studies have been conducted to understand the behavior of soft soils under preloading. An appropriate constitutive model is

a necessity for such purpose, so as to correctly represent the stress state of the soil. Governing equations given by Biot (1941) [18] are generally used for modelling consolidation problems.

Various FEM packages like PLAXIS, ABAQUS and SAGECRISP are available to predict the field variables accurately. Such studies have been carried out in the past and are being developed further to give the results as close to field results as possible. FDM software FLAC is also one of the diverse software used for numerical study of vacuum consolidation.

Because of computational constrains in previous years, numerical studies began with the study of single drain. Then conversion methods of axisymmetric models to plane-strain models were discussed [19, 20]. Hird et al. (1992) [19], converted an axisymmetric unit cell into a plane-strain model. Geometry and average degree of consolidation were the two criteria considered for the conversion. Difficulty in obtaining an acceptable prediction of pore water pressure dissipation was reported in this study, although the settlement predictions were agreeable.

Indraratna and Redana (2000) [21], carried out a plain strain analysis for two case histories in Thailand and Malaysia. It was shown that inclusion of smear zone improves accuracy of predictions. It was also observed that well resistance is only effective enough for PVDs of deeper penetration depth. In addition, Indraratna et al. (2005) [20] have presented a method to transform horizontal permeability from axisymmetric condition to plane strain condition using a modified consolidation theory for vacuum preloading (Figure 2.5). Analytical Solution is developed considering smear zone as well as not considering it. The solutions consider the vacuum pressure to be either constant or linearly varying along the drain as well as across the soil. For closer spacing of PVDs (i.e. 1.0 m), it was observed that predictions with constant vacuum pressure across the soil and linearly varying vacuum pressure along the drain were in agreement with the field results.
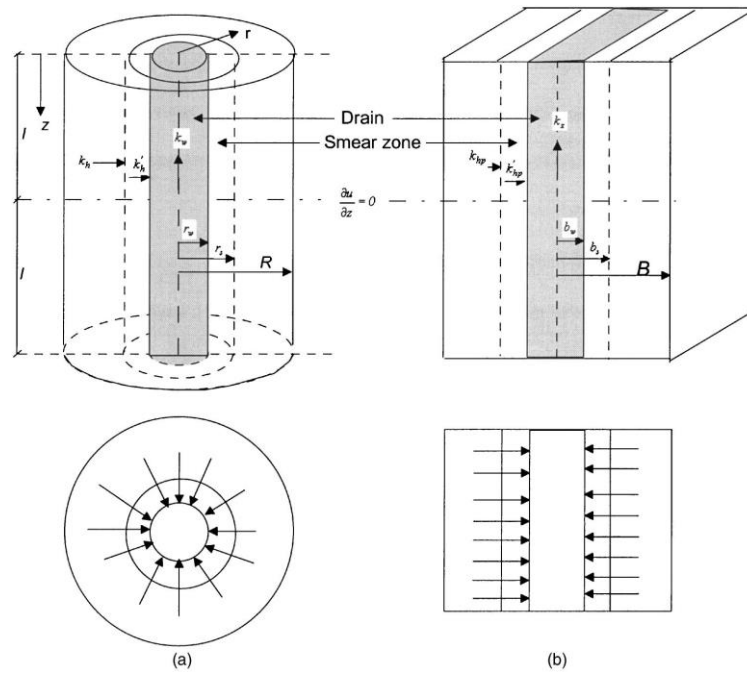
Figure 2.5: Conversion of axisymmetric unit cell into plane strain wall: (a) axisymmetric; and (b) plane strain [20]

Rujikiatkamjorn et al. (2008) [22], presented a 2D and 3D multi-drain analysis coupled with Biot's consolidation theory for modelling vacuum consolidation using FEM software ABAQUS. Combined vacuum and fill loading was considered in this study. Constant pressure was assumed along the drain length based on a field data. The numerical results were compared with the previously obtained field results. It was established that equivalent plane strain method is sufficient for multi-drain analysis using surcharge or vacuum preload.

Later, Witasse et al. (2012) [23] carried out a numerical study on a port reclamation project in Vietnam using PLAXIS 2D under fully coupled flow deformation framework. Capability of FEM to model vacuum consolidation was highlighted. Effective stress, total stress and pore water pressures predicted were found to be close to the field observation. Factor of safety of the fill slop showed a rough increase of 53 to 130 % during construction phase.

2.6 Case Studies on Vacuum Preloading

Several case studies have been carried out in order to understand the field behavior of vacuum assisted consolidation [24-28] apart from the numerical and laboratory studies.

Atmospheric pressure was considered as a temporary surcharge by Kjellman (1952) [10]. Philadelphia International Airport saw the first application of vacuum consolidation in a runway extension project. A temporary stabilization of a soil slope before 1952 using the similar method was also reported by Kjellman.

Chu et al. (2000), [24] presented a case study on vacuum consolidation for an oil storage station in China. In this study, 85 kPa of vacuum pressure was applied to soft soil up to m of depth. Tension cracks were observed on the ground at the treatment area perimeter. A 2 to 3-time increase in undrained shear strength was reported (Figure 2.6).
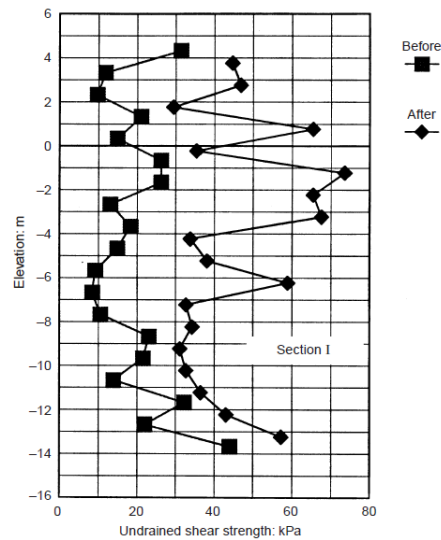
Figure 2.6: Field vane shear results measured before and after vacuum preloading (Chu et al., 2000)

Tang and Shang (2000) [25], presented a case study on Vacuum consolidation for construction of Yaoqiang airport runway. Major challenge was the presence of a silty sand layer of 2-3 m thickness at the surface. Effectiveness of vacuum pressure application was increased by providing deep mixing slurry cut off wall with reduced coverage area of vacuum pumps.

Chu and Yan (2005) [4], proposed a new method for calculation of Degree of Consolidation (DOC) based on pore water pressure profile. This expression was used for calculating DOC for two case studies in China and results were found to be in agreement with those obtained from settlement data.

$$U_{avg} = 1 - \frac{\int [u_t(z) - u_s(z)]dz}{\int [u_0(z) - u_s(z)]dz} \qquad (6)$$

$$u_s = \gamma_w z - s \ (kPa) \qquad (7)$$
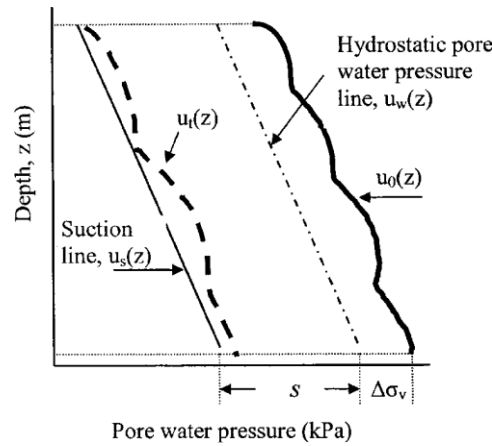
Figure 2.6: Pore water pressure distribution verses depth under combined surcharge and vacuum load [4]

Indraratna et al. (2011) [26], reported a case study at port of Brisbane, Australia where reclamation of land was carried out using dredged material from seabed. It was observed that excess pore water pressure dissipation was higher in vacuum treatment area than in non-vacuum area. It was shown that the lateral deformations were very low below the depth of 10 m. Vacuum combined surcharge was observed to accelerate radial consolidation and control the lateral displacement.

Kumar et al. (2015) [27], presented a case study on the first vacuum consolidation trial in India at Kakinada Port, Andhra Pradesh, India. A square area of 10 m x 10 m was considered for the study. It was observed that the settlements obtained after 28 days of vacuum pressure application were less than those expected. The results indicated that the

17

area was not properly sealed at the perimeter. Also, some sand seams might be present in the treatment soil at some depth which lead to reduction in vacuum pressure. Despite low efficiency, there was an increase in cone penetration resistance because of decrease in water content.

Herve (2015) [28], presented a case study on construction of deep water ports along Cai Mep river in Vietnam. Vacuum pressure of 65 kPa was used along with a surcharge fill of 6.7 m height. The loading sequence was presented with calculation of increase in undrained shear strength at each stage. The improvement in soil properties were demonstrated through the increase in shear strength by a factor of 1.5 up to a depth of 20 m.

2.7 Summary

A review of the literature on preloading, vertical drains, mechanism, laboratory studies and case studies relevant to vacuum preloading technique and physical and numerical modelling of vacuum preloading technique were presented in this chapter. The following findings have been observed from the past studies.

1. Vacuum preloading is a widely used technique for improvement of soft soils.

2. Vacuum preloading eliminated the possibility of bearing capacity failure, hence it is preferred over conventional surcharge preloading

3. The effectiveness of vacuum preloading is influenced by various factors such as drain spacing, leakage in airtight membrane, presence of sand seams in the subsoil

4. Vacuum preloading is an isotropic consolidation process, which also causes inward lateral movement, which can be balanced by using combined surcharge and vacuum preloading.

5. Numerical models can be successfully used in the study of ground improvement by vacuum preloading.

6. 2D numerical models can be conveniently used instead of 3D models when plane strain conditions are more prominent to save computation time.

The literature survey clearly shows that there has been a wide spread research on the vacuum preloading technique in various geotechnical applications like land reclamation and transportation projects. Another observation that can be figured out from this literature study is that most of the numerical studies on vacuum consolidation focused on pore water pressures and settlements during vacuum consolidation. Very less information is available on behavior of soil after vacuum is turned off. The time taken to achieve the required vacuum pressure is also not generally considered in the analysis. In the following chapters the influence of vacuum pressure on consolidation properties of soft clays are studied using PLAXIS 2D numerical model.

Chapter 3

Vacuum Consolidation Model Development and Validation

3.1 Introduction

Thera are many programs available for numerical analysis of geotechnical processes, like PLAXIS, ANSYS, ABAQUS and FLAC. The first three are finite element based programs while FLAC is a finite difference based program. Numerical methods help us resolve the complexities like boundary effects, scale effects, material anisotropy, non-linear behavior, field stress conditions.

Many researchers have modelled vacuum consolidation using finite element methods (FEM). Rujikiakamjorn et al. (2008) [6] modelled Vacuum preloading system in ABAQUS coupled with Biot's consolidation theory and concluded that an equivalent plane strain analysis is sufficient for multi-drain analysis of large projects. Wu and Hu (2013) [29], demonstrated the superiority of modelling a cube drain over the cylindrical drain, but considering the convenience in theoretical analysis, the cylindrical drain may be preferred. Indraratna et al. (2005) [20] presented a modified consolidation theory and used ABAQUS to demonstrate the effect of magnitude and distribution of vacuum pressure along the drain and across the soil.

Later, Witasse et al. (2012) [23] carried out a numerical study using PLAXIS 2D under coupled flow deformation framework for a port reclamation project at Vietnam and found that the results were in agreement with the previously calculated results. Indraratna et al. (2016) [30] used PLAXIS to model a trial test embankment in Ballina, Australia and

demonstrated the capability of FEM in obtaining optimum time for application of vacuum pressure.

3.2 Finite Element Method (FEM)

The finite element method is a numerical procedure for analyzing structures and continua. Initially developed to solve the problems related to stress analysis, the finite element method has been developed to analyze problems of heat transfer, fluid flow, lubrication, electric and magnetic fields etc. FEM divides the structure into several elements, then reconnects the elements at the nodes. Then, stress and strains are calculated in those elements and those elements are then joined using the principle of superposition.

Use of FEM for geotechnical engineering dates back to 1966, when it was first used to determine stresses and strains in embankments (Clough and Woodward, 1967) [31] and analysis of underground openings in rocks (Reyes and Deene, 1966) [32]. Almost all geotechnical problems can be modelled in finite time steps which describe sequence of real time events. This helps in changing the geometry along with the soil properties with each step to simulate the changes in stress state within the soil mass.

3.3 PLAXIS 2D Software

PLAXIS 2D is a multi-purpose two-dimensional finite element program used to perform deformation, stability and flow analysis for various types of geotechnical applications. Various applications include static elastoplastic deformation, advanced soil models, stability analysis, updated mesh, consolidation, steady-state ground water flow, safety analysis and consolidation. Plane strain and axisymmetric models are available to simulate real situations. Besides, convenient graphical user interface enables quick generation of geometry and finite element mesh based on dimensions of the model provided.

3.4 Fully Coupled Flow Deformation Analysis

A Fully Coupled Flow-Deformation analysis is conducted when it is necessary to analyze the simultaneous development of deformations and pore pressures in saturated and partially saturated soils as a result of time-dependent changes of hydraulic boundary conditions. The rate at which consolidation occurs in saturated soil is determined by the rate at which the

pore fluid can flow out of the soil [18]. This analysis operates on total pore pressure, i.e. the sum of steady state and excess pore pressures. Steady-state pore pressures are calculated at the end of calculation phase based on hydraulic conditions. Fully coupled flow-deformation analysis considers the unsaturated behavior of soil, when necessary and incorporates suction in unsaturated zone above the phreatic level. Instead of excess pore pressure, the method acts on total pore pressure which is the sum of steady state and excess pore pressure. This procedure finds application in rapid drawdown problems, vacuum consolidation modelling, embankment dams subjected to tidal forces and consolidation problems.

Biot (1941) [18] presented the formulation of coupled consolidation behavior of soils. The governing equations for the coupled consolidation:

Effective stress principle $$\sigma = \sigma' + p_w \tag{3.1}$$

Transient flow equation $$v - \dot{\varepsilon} = 0 \tag{3.2}$$

Darcy's law $$v = Kh \tag{3.3}$$

$$h = (x - x_D) + \frac{p_w}{\gamma_w} \tag{3.4}$$

Where, σ = total stress, σ' = effective stress, p_w = pore water pressure, v = the gradient of the velocity of the pore fluid, $\dot{\varepsilon}$ = the volumetric strain rate, K = permeability matrix, h = potential energy head of the pore fluid, x = direction of gravity and x_D = datum plane elevation.

3.5 Elements used in the study

Finite element considers the continuum as formed by a number of elements, each consisting a number of nodes. Number of degrees of freedom (DOF) are defined at each node which consist of the unknowns needed to solve the boundary value problems. In deformation problems, the DOF are the displacements at nodes while in flow analysis, DOF are groundwater heads. This section covers the elements used to capture the vacuum consolidation behavior

15-noded triangular elements: 15-noded triangular elements (Figure 3.1) fall under the category of area elements, used to model surface and soil mass under plane strain conditions. These elements provide fourth order interpolation for displacements and twelve stress (Gaussian) points for stress calculations. In FEM formulations, local coordinates ξ and η are available for triangular elements; besides, auxiliary coordinate $\zeta = 1 - \xi - \eta$, is also added for better interpolation (local numbering and position of nodes is shown in Figure 3.2).

Figure 3.1: Position of nodes and stress points in 15-noded triangular element

The shape functions of the 15-noded triangular element are as given below:

$N_1 = \zeta(4\zeta - 1)(4\zeta - 2)(4\zeta - 3)/6$

$N_2 = \xi(4\xi - 1)(4\xi - 2)(4\xi - 3)/6$

$N_3 = \eta(4\eta - 1)(4\eta - 2)(4\eta - 3)/6$

$N_4 = 4\zeta\xi(4\zeta - 1)(4\xi - 1)$

$N_5 = 4\xi\eta(4\xi - 1)(4\eta - 1)$

$N_6 = 4\eta\zeta(4\eta - 1)(4\zeta - 1)$

$N_7 = \xi\zeta(4\zeta - 1)(4\zeta - 2)*8/3$

$N_8 = \zeta\xi(4\xi - 1)(4\xi - 2)*8/3$

$N_9 = \eta\xi(4\xi - 1)(4\xi - 2)*8/3$

$N_{10} = \xi\eta(4\eta - 1)(4\eta - 2)*8/3$

$N_{11}=\zeta\eta(4\eta - 1)(4\eta - 2)*8/3$

$N_{12}=\eta\zeta(4\zeta - 1)(4\zeta - 2)*8/3$

$N_{13}=32\eta\xi\zeta(4\zeta - 1)$

$N_{14}=32\eta\xi\zeta(4\xi - 1)$

$N_{15}=32\eta\xi\zeta(4\eta - 1)$
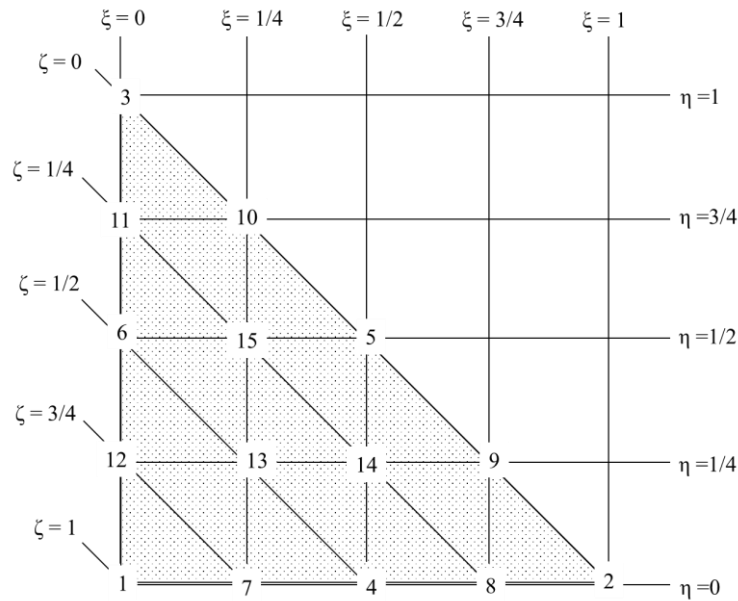
Figure 3.2: Local numbering and position of nodes in a 15-noded triangular element

Drains: Drains are considered seepage boundaries, located inside the soil mass (model domain). The excess pore water pressure along the drain is zero allowing the water to leave the model at atmospheric pressure.

3.6 Load Stepping Procedure

Analysis of plastic soils involve non-linear equations; thus, problems need to be solved in a series of steps. A step size and calculation algorithm can be defined accordingly. Equilibrium errors are successively reduced during each calculation step using a series of iterations. Optimum step size will limit the number of iterations. Small step size induces large number of steps to reach desired load level, increasing computation time. On the other hand, a too large step size may cause the solution to diverge as the number of steps may

become excessive. PLAXIS has an automatic load stepping procedure for solution of non-linear plasticity problems. The automatic procedure maintains a balance between the robustness, accuracy and efficiency.

3.6.1   Critical Time Step

Accuracy increases with reducing the time step; however, for consolidation problems there exists a threshold value below which a rapid decline in accuracy is observed. The critical time step is calculated as

$$\Delta t_{critical} = \frac{H^2}{\eta \alpha C_v}$$

(3.5)

Where C_v is the coefficient of consolidation, H is the height of the element, α is the time integration coefficient and η is a constant parameter which depends on type of element.

3.7 Material Models

To model mechanical behavior of different soils, we need material models which would accurately define the behavior of material under different loading conditions. Depending on the complexity of the problem we can select appropriate model to capture essential features of soil and rock behavior. Marine clay in the study is assumed to follow the Soft Soil Model which is a cam-clay type model, ideally suited for primary compression problems. Soft soil model has linear stress-dependency for soil stiffness (Figure 3.3). Any point on this normally consolidated line represents the stress state for the soil.
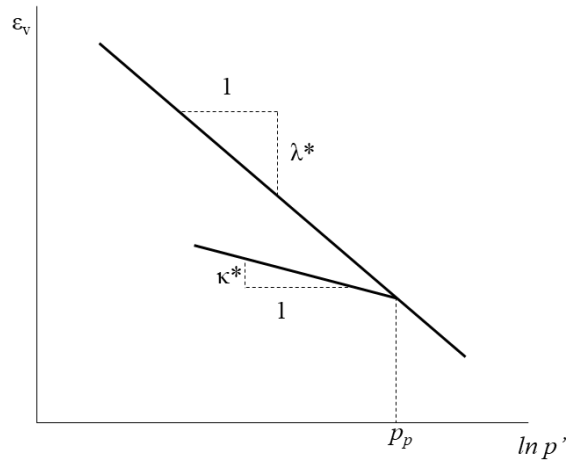
Figure 3.3: Logarithmic relation between volumetric strain and mean stress
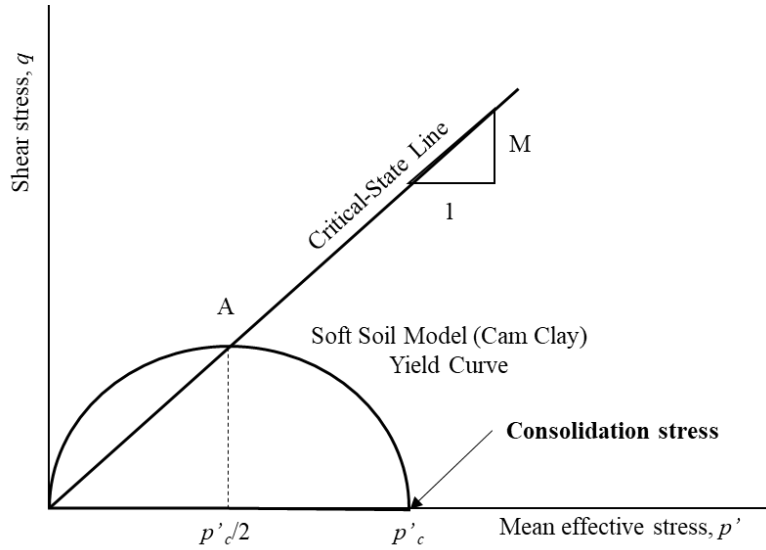
Figure 3.4: Critical State line and yield curve in *p'-q* space

The yield function of the model describes an ellipse in p'-q space (Figure 3.4). The equation for ellipse is given by

$$\frac{q^2}{p'^2} + M\left(1 - \frac{p'_c}{p'}\right) = 0 \qquad (3.6)$$

The slope of critical state line (CSL) can be found as

$$M = \frac{6\sin\phi'}{3 - \sin\phi'} \qquad (3.7)$$

26

Various material parameters include modified compression and swelling indices, as well as Mohr-Coulomb model failure parameters.

Modified compression index (λ^*): The slope of primary loading line is termed as modified compression index. The relation between original cam-clay parameter λ and C_c is given as

$$\lambda^* = \frac{\lambda}{1+e} = \frac{C_c}{2.3(1+e)}$$

(3.8)

Modified swelling index (κ^*): The slope of unloading/swelling line gives modified swelling index. The relation between original cam-clay parameter κ and C_c is given as

$$\kappa^* = \frac{\kappa}{1+e} \approx \frac{2C_s}{2.3(1+e)}$$

(3.9)

Cohesion: As illustrated in Figure 3.4, cohesion results in an elastic region which lies partly in tension zone. It is always specified as an effective stress parameter and should not be zero.

Friction angle: It is recommended to use critical state friction angle, based on small strains.

Poisson's ratio: A default value of 0.15 is available for general calculations. Contribution of Poisson's ratio is not significant for primary loading problems; however, it gains importance in unloading conditions.

3.8 Boundary Convergence study

In comparison with the reality, boundaries are actually non-existent, and their selection needs to be done that they do not actually influence the behavior of the problem to be modelled. In particular, boundaries have to be 'far away'. The question of how far we need to provide the boundaries is answered by the Boundary Convergence Study, as it provides a balance between calculation time and accuracy. Boundaries too close will induce boundary effects whereas boundaries located too far will increase the calculation time. The boundary distance after which there is significant change in the resulted settlement shall be considered as the optimum boundary distance. Boundaries can be completely free or fixities can be applied in one or two directions.

3.9 Boundary Conditions

The boundary conditions include allowed displacements and flow conditions at the boundaries of the model. In this study, the bottom of the soft soil is underlain by stiff clay layer and top is overlain by fine sand layer. Horizontal boundaries are kept free to move in the vertical direction (roller support). The boundary conditions are as given in Table 3.1.

Table 3.1: Boundary conditions in the soil model

Boundary	Seepage	Displacement
Left	Open	Roller
Right	Open	Roller
Top	Open	Free
Bottom	Closed	Fixed

3.10 Mesh sensitivity study

Mesh sensitivity study is carried out to fix the size of elements on the basis of relative element size factor (r_e'). Target element size (I_e) in PLAXIS is dependent on the overall model geometry and is given by the following expression:

$$I_e = r_e \times \sqrt{(x_{max} - x_{min})^2 + (y_{max} - y_{min})^2} \qquad (3.10)$$

Value of r_e can be any one among 2.00, 1.33, 1.00, 0.67 and 0.50 corresponding to very coarse, coarse, medium, fine and very fine element distribution. Having a finer mesh will result into a better distribution of stresses and strains across the domains, but it will add excessively to the computation time.

3.11 Vacuum Consolidation in PLAXIS 2D

Vacuum consolidation is applied in almost saturated soil with high ground water table (GWT). The technique uses atmospheric pressure as a preload. Since, PLAXIS does not take air pressure into account, the application of vacuum pressure is modelled by reducing the groundwater head in drains. The excess pore pressure along the drains is zero otherwise, thus reducing the ground water head will create the head difference necessary for water to

flow into the drains. This negative ground water head cannot exceed 10 m below the GWT, which is equivalent to the atmospheric pressure of 100 kPa.

Reducing ground water head in drains will lower the groundwater head throughout the area which would result into the soil becoming unsaturated leading to a change in permeability of the soil mass. However, since in reality, the global water level doesn't drop, this change in permeability is unrealistic and should not happen. Thus, in material model parameters, saturated and unsaturated unit weight should be kept equal. Besides, to avoid reduced permeability, hydraulic model is set to saturated in ground water flow datasheet. To consider the suction pressures which are generated because of decrease in phreatic level, ignore suction option is selected in phase calculation window.

3.12   Validation with Case Study of Reclamation Project in Vietnam

3.12.1 Introduction

After a numerical model is developed, it is necessary to validate the results with available studies in literature. A finite element analysis performed for a reclamation project in Vietnam for construction of container port ([23, 28]) along Cai Mep river was considered for validation. The region had weak soft soil up to a depth of 40 m. Large settlements were anticipated during and after the construction period. Thus, a need for ground improvement was sought.

3.12.2 Numerical model

The finite element mesh was generated under plane strain conditions using 15-node triangular elements. The mesh spanned 450 m in horizontal and 135 m in vertical direction. The mechanical and hydraulic boundary conditions are shown in Figrure3.3. Full model was considered instead of half model because of asymmetry. The top and horizontal boundaries were kept close to seepage. The bottom boundary is kept fixed, horizontal boundaries are provided roller support conditions and top boundary is kept free for displacement. The node and stress points selected for calculation are as shown in Figure 3.6.
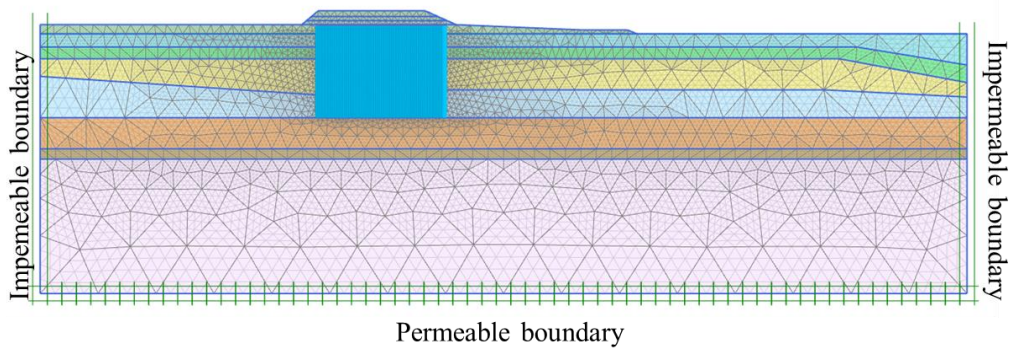
Figure 3.5: Generated Finite Element Mesh in PLAXIS 2D for vacuum consolidation at port reclamation project in Vietnam
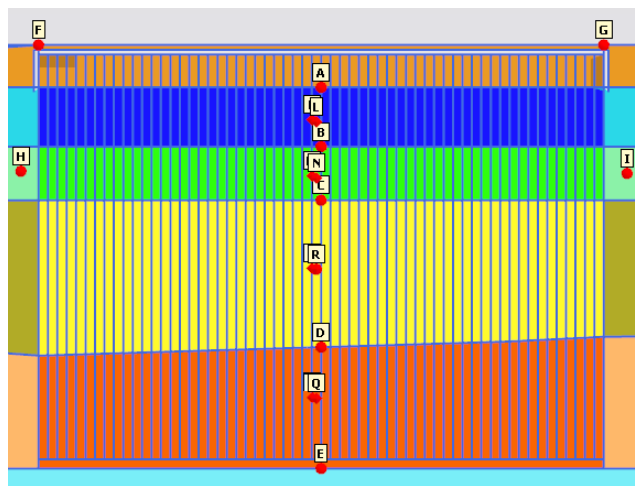
Figure 3.6: Points for calculation of displacements and stresses (A-E: nodal points, K-N: stress points), (adopted from Witasse et al, 2012 [23])

The settlements obtained with time at different depths are shown in Figure 3.7. As anticipated in the study, the settlements are very high and this reinforces the need for ground improvement. Figure 3.8 compares the active pore pressure obtained in the present study with the results in the previous study. It was found that the data was in good agreement with the already published result.
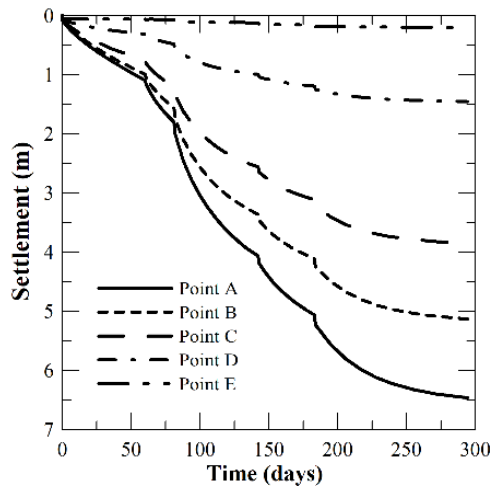
Figure 3.7: Settlements at reclamation project in Vietnam
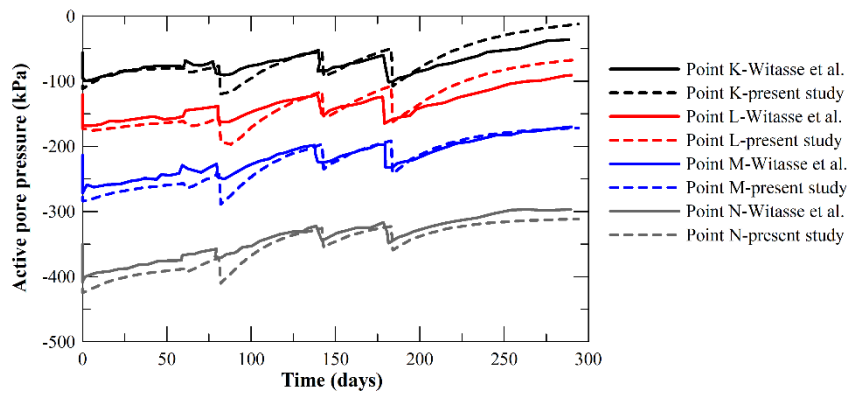
Figure 3.8: Pore water pressures at reclamation project in Vietnam

3.13   Summary

A numerical model capable of simulating the behavior of vacuum consolidation appropriately was formulated in this chapter using PLAXIS 2D software. Fully coupled flow-deformation analysis was employed under plane strain conditions to predict the settlement and pore water pressures. Boundary convergence and mesh sensitivity analyses were discussed to fix the model horizontal boundaries and element size in mesh. The model was validated with the available case study at Vietnam port reclamation project and observed that the settlements and pore pressures were in good agreement with the published results. This study highlighted the capability of PLAXIS 2D to model vacuum consolidation under plane strain framework.

Chapter 4

Study of Vacuum Consolidation in Kakinada Coastal Clay Deposits

4.1   Introduction

Kakinada is situated on the eastern coast in the state of Andhra Pradesh, India. The port region has soft clay deposits of thickness 10-11 m. The area is becoming a trade hub because of presence of Kakinada port and there is a need for improvement of soil to support important infrastructure facilities.

4.2   Field study at Kakinada Port

First field trial of vacuum consolidation in India was carried out by Kumar et al. (2015) [27] in Kakinada soft clay deposits. The foundation soil in this region is characterized by the presence of thick layers of soft marine clay deposits. In view of increasing demand for development of fertilizer plants and ports, a need for ground improvement was sought. A square area of 10 m x 10 m was considered for study. Because of cyclonic disturbances the test could not be conducted beyond 28 days [27]. It was observed that the settlements obtained after 28 days of vacuum pressure application were less than those expected from laboratory studies. Many parameters like pore pressure, lateral displacement, and loss of vacuum pressure in the field could not be measured; however, if predicted, can be of great help in studies of soft clay deposits. In this study, Plaxis 2D software is used to model the field trial and the numerical results obtained have been compared with the field data.

General Description of Site Conditions and Soil Characteristics

The site of field trial is located at Kakinada coast, Andhra Pradesh, India. Standard Penetration Test results showed that the first 3m of the soil strata was fine sand (Figure 4.1), followed by 10.5 m of very soft marine clay with SPT value 1 and natural water content of

84% [27]. Soil below 14m was very stiff clay with SPT value of 50. Ground water table was present at 0.5m below the ground level. Study of undisturbed core samples collected at the depth of 10.5m showed that the marine oft soil was found to be fine grained and classified as OH soil as per Indian Soil Classification System and Rao et al. (2011) [33]. The soil properties mentioned in the referred literature and adopted or calculated from given data are presented in Table 5.1.
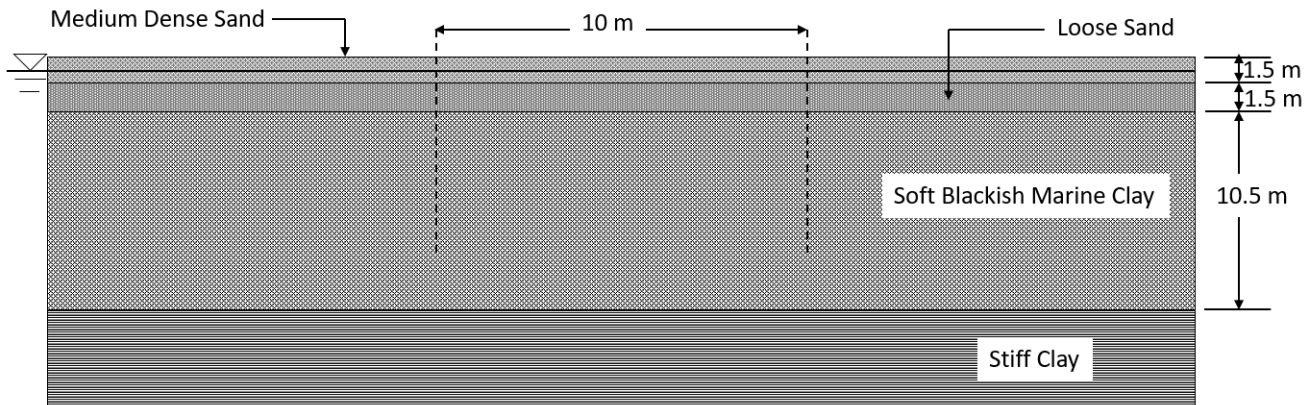
Figure 4.1: Soil profile of treatment area

Table 4.1: Adopted model parameters for the study

Property	Unit	Value
Unsaturated unit weight#	γ_{unsat} (kN/m³)	16.00
Saturate unit weight#	γ_{sat} (kN/m³)	16.00
Initial void ratio	e_{init}	1.76
Modified compression index##	λ^*	0.09450
Modified swell index##	κ^*	0.01120
Compression index	C_c	0.6
Recompression index	C_r	0.083
Secondary compression index	C_s	0.036
Cohesive strength#	c_{ref} (kN/m²)	3.5

Angle of internal friction#	Φ (°)	2.0
Coefficient of horizontal permeability##	k_x (m/day)	3.615E-05
Coefficient of vertical permeability##	k_y (m/day)	6.245E-05

assumed   ## calculated from available data

4.3 2d Plane Strain Finite Element Model

The geometry of field trial was simulated using the finite-element software PLAXIS 2D. The soil properties obtained from the laboratory tests (Table 5.2) along with the adopted properties were used to model the behavior of the test section. Soft soil model has been considered for the clay layer. Material properties have been defined in terms of effective stiffness and effective strength parameters. Undrained behavior has been assumed for soft clay layer. Fully coupled flow deformation is employed to analyze the given soil model with unsaturated soil condition. A fully coupled flow deformation is conducted when it is necessary to analyze the simultaneous development of deformations and pore pressures in saturated and partially saturated soils as a result of time-dependent changes of the hydraulic boundary conditions. The model has been set-up in plane strain situation using 15-nodes triangular elements which provide a high order of displacement and pore pressure interpolation.
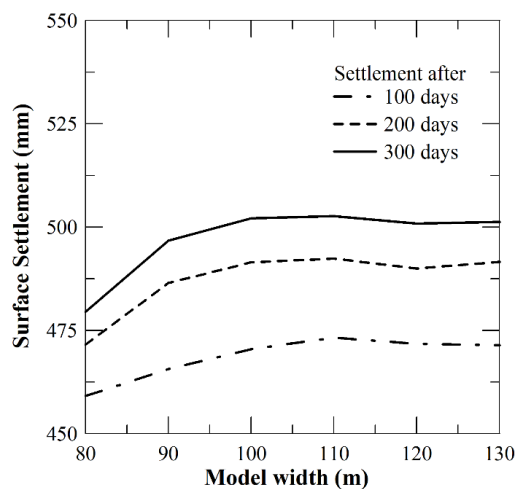
Figure 4.2: Boundary Convergence Study for development of 2D model

Boundary convergence study was carried out to decide the extent of the horizontal boundaries of the model (Figure 4.2). After the distance between two boundaries exceeded 100m, no significant change in settlement was observed. So, soil model of width 100m and depth 18m was created in PLAXIS 2D including a 4.5m of stiff clay layer below the marine clay layer to maintain one-way drainage. Vacuum preload was modelled in an area 10m wide at the center of the model. The PVDs were modelled as drain elements. The PVDs were modelled as linear drain elements. A drain blanket of 0.2m height is provided over vacuum treatment area.

Table 4.2: Sensitivity study of 2D model in PLAXIS 2D

Mesh refinement	Relative element size factor (r_e')	Coarseness factor	no. of elements	no. of nodes	settlement at 300 days (mm)	ultimate settlement (mm)
very coarse	2	0.25	817	6723	500.2	601.9
coarse	1.5	0.25	826	6813	500.6	602.4
medium	1	0.25	857	7079	501	603
fine	0.67	0.25	1186	9761	502.14	604.7

Sensitivity study was conducted to analyze the effect of element size and on results. Four types of mesh were generated: Very Coarse, Coarse, Medium and Fine. Fineness of mesh is varied by changing Relative Element Size Factor (r_e'). Values for this parameter are given in Table 3.
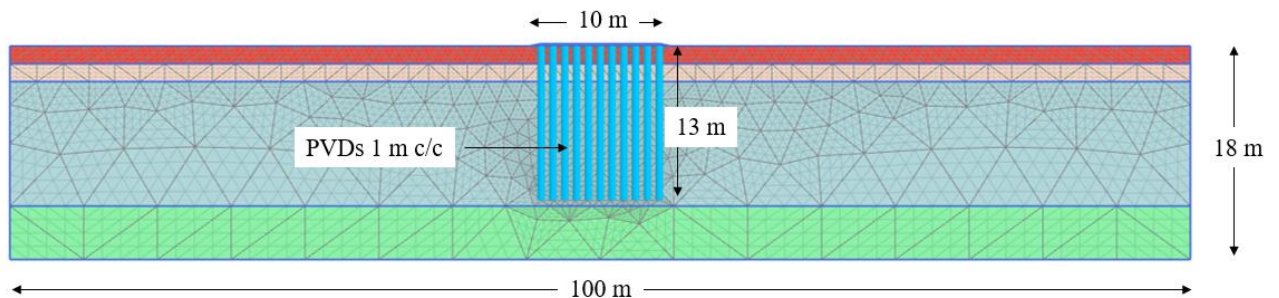
Figure 4.3: 2D Finite Element Mesh generated for the analysis

Another parameter called Coarseness Factor is used to refine the mesh locally at drains. Finer meshes are helpful when the behavior of very closely situated points is to be studied. It was found that the settlement was same for all the four types of meshes. Fine coarseness was finally adopted and the mesh is shown in Figure 4.3. The vacuum pressure is specified by the negative water head along the length of the drains (a reduction of groundwater head of 10m signifies under-pressure of 100kN/m², i.e. complete vacuum). To apply saturated conditions in the soil volume, the unsaturated unit weight was made equal to the saturated unit weight. Otherwise, reduction in groundwater head in vertical drains would drop the phreatic level, thus resulting into change in unit weight of soil. Nodal point to calculate displacement was selected at the center of treatment area. Stress point for stresses and pressures was selected at the center of treatment area at mid depth of clay layer very near to the drain and also between two adjacent drains. The left and right flow boundaries were kept open. Bottom flow boundary was closed to seepage to maintain undrained conditions.

4.4 Results and Discussions

Settlement

For field works involving ground improvement, vacuum load is applied for generally 7-9 months. Since 80-93 kPa vacuum pressure was applied in the field trial, vacuum pressure of 85 kPa was applied in the numerical model for 300 days and then stopped. The soil model was then further observed for 30 days without vacuum pressure.

Figure 4.4: Comparison of field data with numerical results under different vacuum pressures

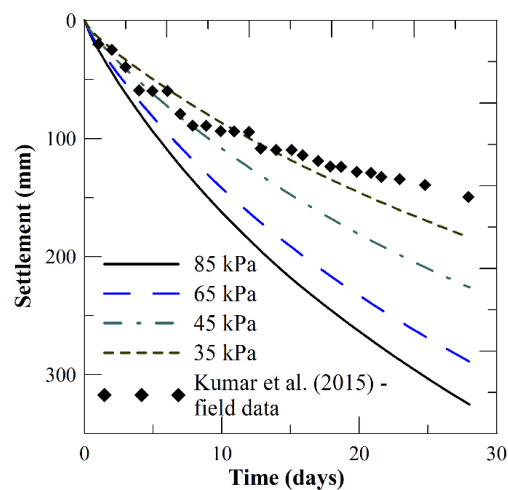In 28 days 333 mm of settlement was observed in numerical model. While in 300 days the settlement reached 501 mm. When the water head in drains was restored, i.e. vacuum was stopped, the soil showed a little rebound of 25 mm. This shows that rebound modulus of soil is very low. However, in field only 150 mm of settlement was reported in 28 days, which is very low when compared to the numerical results. The following problems were recognized by Kumar et al (2015) [27] during the field trial:

1. Presence of thin sand seams in the ground, providing extra drainage path to the pore water

2. The test area was not properly sealed and was in close proximity of the sea shore, allowing the continuous entry of water from the sides.

3. Actual vacuum pressures developed in the foundation soil could not be measured.

This also shows that short duration field tests may not be sufficient enough to obtain complete information about soil behavior during vacuum consolidation. For comparison with field observations the model was studied under different vacuum pressures of 55 kPa, 65 kPa and 75 kPa. It is observed from Figure 4.4 that numerical results are not in agreement with field results. It can be concluded that required vacuum pressure could not be maintained in the soil. This is possible if thin sand seams are present in the field. Since numerical model considers isotropic nature for materials and uniform layers of soil, the calculated values of settlements are higher than those observed in field.

To study the loss of vacuum in field, 4 cases were simulated in numerical model. These cases are compared with field data in Figure 4.5. Settlement obtained from Case 1 was too high compared to the field observation. Case 2 resulted in final settlement after 28 days close to field data but the initial settlement profile is steeper. Case 3 resulted in higher settlement after initial few days. Case 4 resulted in settlements in agreement with the field data. It can be concluded that there was a heavy loss of vacuum in the field trial and only 30-40% of vacuum applied was able to reach the treatment area.

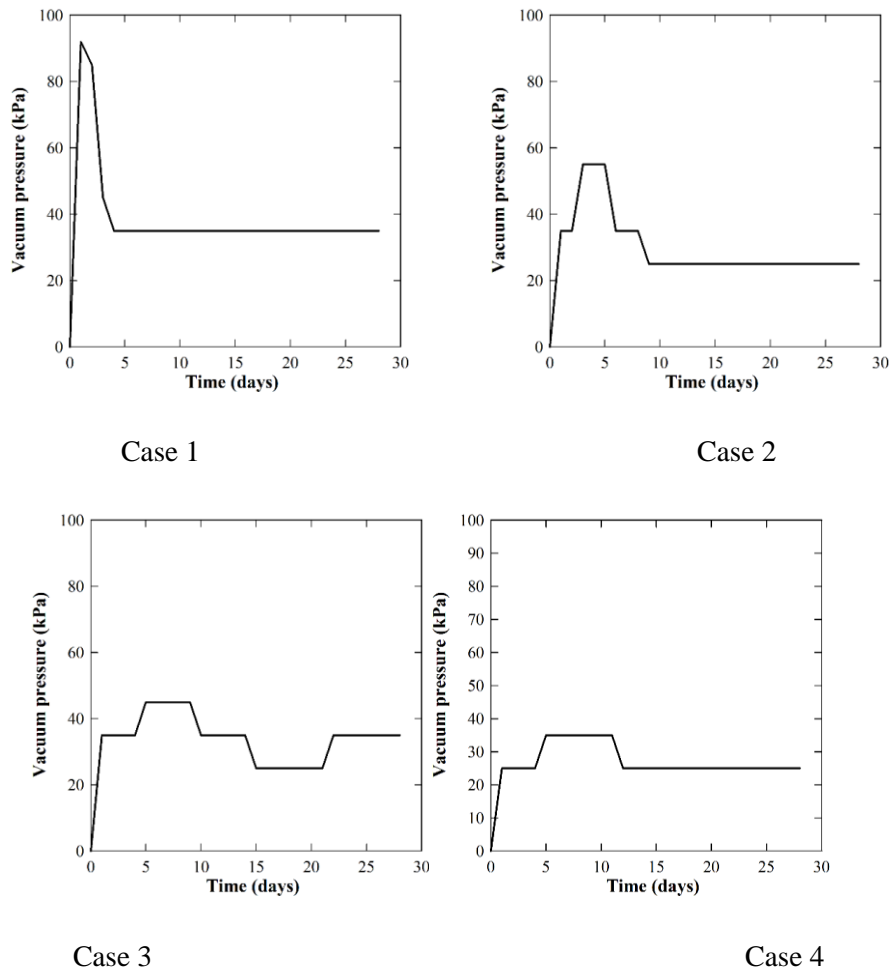Case 1   Case 2

Case 3   Case 4

Figure 4.5: Four cases for vacuum dissipation considered in study
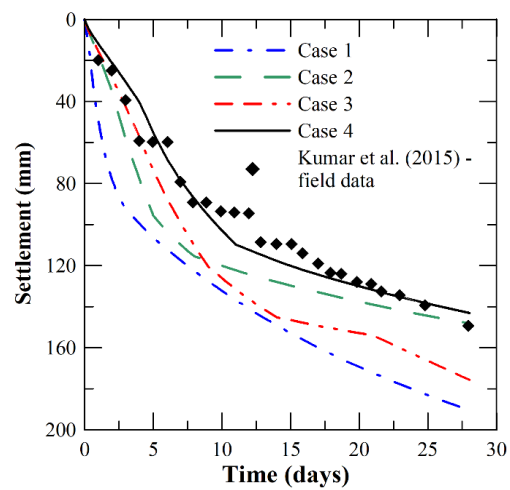

Figure 4.6: Settlements under different VP loss case studies

Hyperbolic method [34] was used to predict the ultimate settlement using the 28 days' data obtained in numerical study using Case 4 and it was observed that the final settlement after 200 days was 225 mm, which in agreement with the predictions from field observations [27] (Figure 4.7).
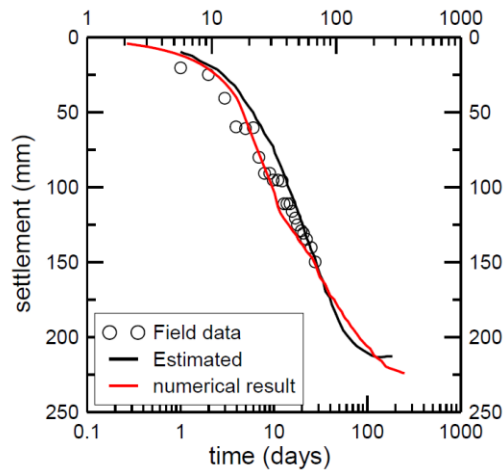
Figure 4.7: Comparison of estimated results from field and numerical analysis

Pore Water Pressure

One of the major parameters affecting the consolidation process is the change in pore pressure. Application of vacuum reduces the pore pressure in treatment area. Pore pressure reduction at mid depth of clay layer for Case 4 (Figure 4.5) as well as without any vacuum pressure (VP) loss is shown in Figure 4.8. It can be observed that pore pressures reduce by the amount of vacuum pressure applied during the vacuum application period. However, the regions adjacent to the individual drains undergo the reduction very soon as the pressure is applied, but then the rate of reduction in pore pressure slows down after some time. This can be explained by the fact that when consolidation of soil adjacent to the drains take place, pore spaces shrink thus making it difficult for pore pressure to dissipate afterwards. The region between two adjacent drains take time to reach the constant minimum pore pressure stage. Pore pressure in this region increases initially by a small amount, then dissipates. This phenomenon is popularly known as the *Mandel-Cryer effect*. When the pore pressures at the boundary start to dissipate the local deformation may lead to an immediate effect in other parts of the soil body, and this may lead to an additional pore pressure [35].
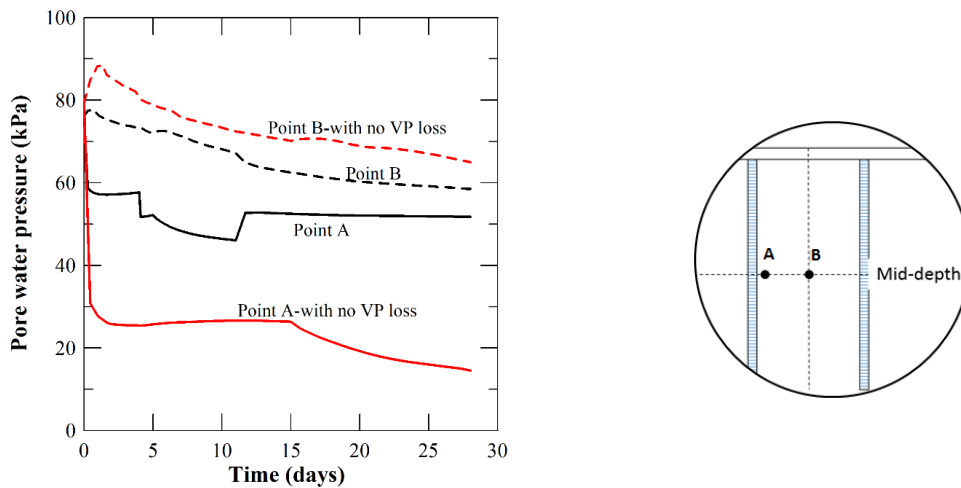
Figure 4.8: Pore pressure time history under Case 4 and vacuum load of 85kPa

Reduction in pore pressures for Case4 at different depths is shown in Figure 4.9. It can be observed that the initial increase in pore is high near top layer of clay strata because of presence of sand boundary. The increase ceases with the depth.
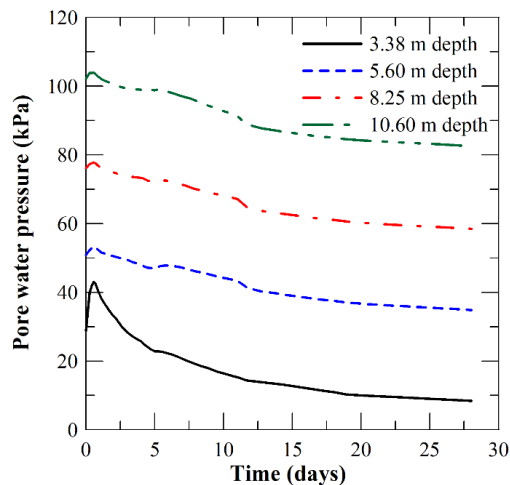
Figure 4.9: Pore pressure at different depths

When the vacuum is switched off, pore pressures do not reach the initial value immediately in the whole treatment area (Figure 4.10(a) & 4.10(b)). Because of consolidation, void spaces get compressed and dissipation of vacuum from soil takes time. The numerical model is not able to predict the proper behavior of pore pressure when vacuum is switched off. A rebound of 20 mm is observed over the next 30days because of removal of stress, indicating that the rebound modulus of the soil is very low.

40
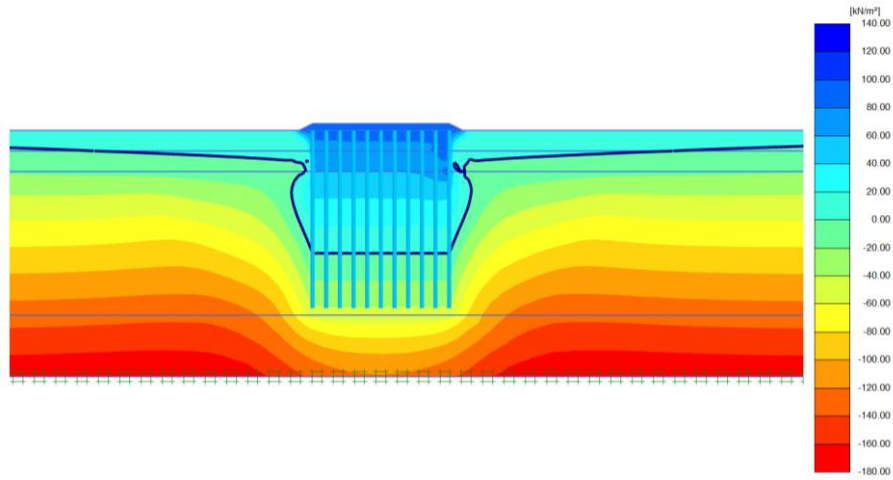
(a)
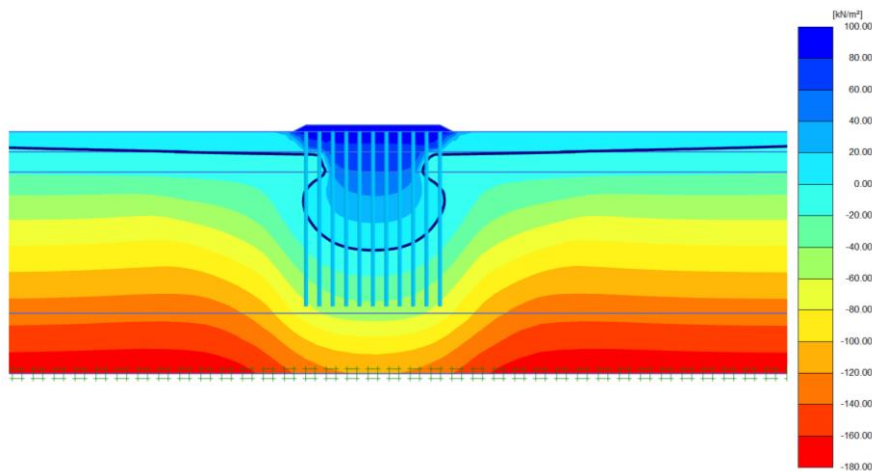
(b)

Figure 4.10: (a) Pore water pressure contours after 300 days of vacuum pressure application (just before switching off vacuum) (b) Pore water pressure contours one day after switching off vacuum

To determine the average Degree of Consolidation (DOC), method suggested by Chu and Yan (2005) [4] was followed. The equation to find DOC is given by:

$$U_{avg} = 1 - \frac{\int [u_t(z) - u_s(z)]dz}{\int [u_0(z) - u_s(z)]dz} \tag{4.1}$$

$$u_s = \gamma_w z - s \text{ (kPa)} \tag{4.2}$$

Where $u_0(z)$ = initial pore water pressure at depth z; $u_t(z)$ = pore water pressure at depth z at time t; $u_s(z)$ = suction line, z =depth; γ_w = unit weight of water; and s = suction applied.

Figure 4.11 shows distribution of pore water pressure with depth in the clay layer at midpoint between two drains at center of treatment area. To calculate average degree of consolidation (DOC), pore pressures at top bottom and mid-depth of the clay layer were considered at the end of vacuum application period. The degree of consolidation, U_{avg} in Case 4(Figure 4.5) in 28 days was calculated to be 76 %. Degree of consolidation calculated using field settlement data was calculated to be 70 %, which is in agreement with the DOC obtained from pore pressure criteria.
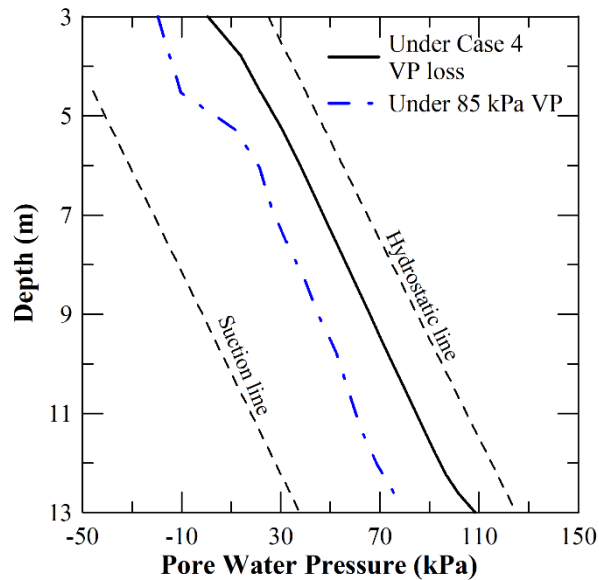
Figure 4.11: Prediction of pore pressure variation with depth in clay soil for field trial and application without vacuum loss

Lateral displacement

The horizontal displacement at the boundaries of soft ground subjected to vacuum loading results from consolidation of the soil, and it is inward to the vacuum-loaded area. (Figure 4.12). Inward displacements are induced due to vacuum pressure exceeding lateral stress required to maintain a k_o condition. The condition for inward lateral displacement to occur can be given as follows (Chai et al 2005) [15]:

$$\Delta\sigma_{vac} > \frac{k_0 \cdot \sigma'_{v0}}{1-k_0}$$

(4.3)

Where k_0 = at-rest horizontal earth pressure coefficient; σ'_{v0} = in situ vertical effective stress; and $\Delta\sigma_{vac}$ = incremental vacuum pressure. The present case satisfies the above criteria.

Maximum value of 120 mm is measured in the soil at the edge of treatment area at a depth of 6 m (Figure 4.12). On a contrary, the maximum inward movement was expected to be at the surface [15]. It was observed that the existing sand layer over the clayey soil prevents the soil from caving in, thus preventing tension cracks. The lateral displacements were found to be majorly confined in the soft soil layer. If the existing strata has clay layer extending from top to bottom, the settlements would be maximum at the surface, forming an inward caving profile. At the surface 60 mm lateral displacement was predicted in this study.
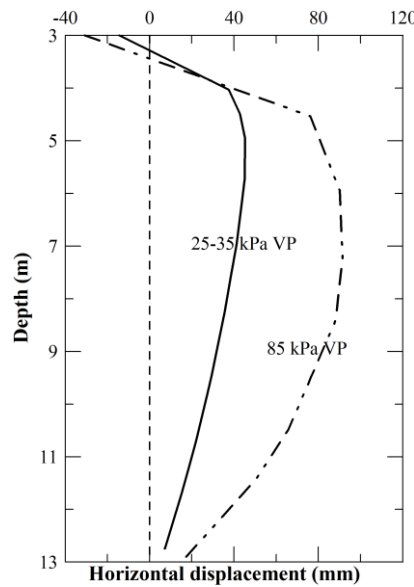
Figure 4.12: Lateral displacements induced in soft clay layer due to vacuum load at left edge

Staged Vacuum Application

The effect of staged vacuum application on the considered marine soil was studied. Instead of applying entire vacuum pressure at one time, pressure was applied in stages. Three cases studies were considered for staged application (Figure 4.13). First, 35 kPa vacuum pressure was applied for 30 days, then 60 kPa was applied for next 30 days (Figure 4.13a). Then 85

kPa pressure was applied. Similarly, 55, 70 and 85 kPa vacuum pressures were applied for second case (Figure 4.13b). In third case, 85kPa was applied after 30 days application of 55kPa pressure (Figure 4.13c). The results show that settlements obtained by all three cases reach the settlement given by single stage application of 85 kPa vacuum pressure (Figure 4.13). So, even if lower vacuum pressure is given in initial period and then required vacuum is build up, same result can be achieved. This may lead to less consumption of power, electric or diesel, eventually leading to economic benefits.

(a)

(b)

(c)

(d)
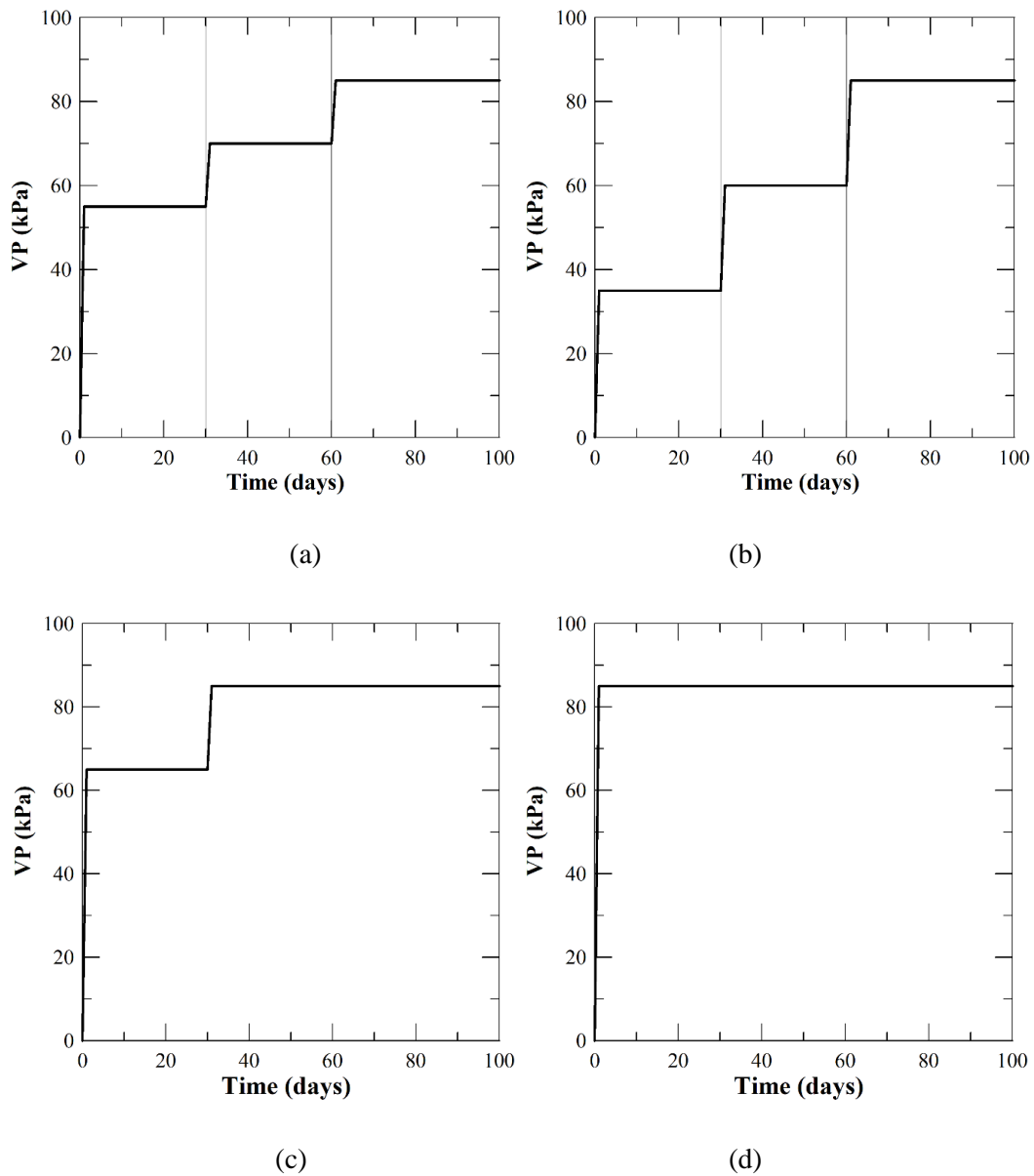
Figure 4.13: Case studies for Staged VP application
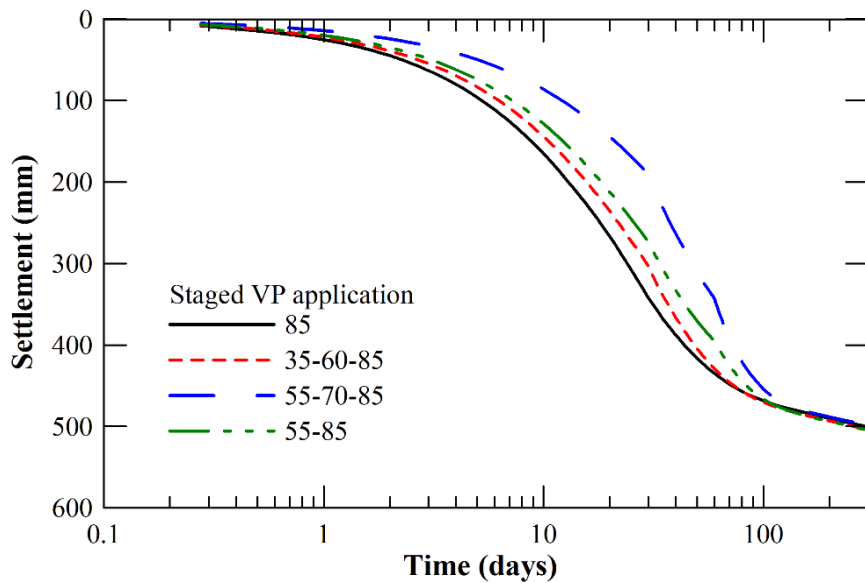
Figure 4.14: Comparison of staged vacuum loads with single stage vacuum load

4.5 Parametric Studies

Influence of Surcharge Preload on Vacuum Consolidation

The behavior of soft soil along with surcharge preload was analyzed in the previous sections considering only the vacuum preload. In this section, effect of surcharge coupled vacuum preload is presented. The influence of time of placing surcharge is considered in this study and the comparisons have been drawn when surcharge is placed before and after the vacuum load is activated. It can be observed from the Figure 4.15 that when surcharge load is placed before the vacuum is activated, the increase in pore pressure will initially be used in reducing the excess pore pressure generated because of the surcharge load. If the soil is very soft, the additional surcharge at the beginning may lead to the shear failure of the soil. On the other hand, if surcharge load is placed after the vacuum load is activated, the soil would have gained sufficient strength by that time and the increase in pore pressure will not cause any failure in the soil mass.

Improvement in Settlement Characteristics after the Vacuum Consolidation Treatment

It is important to assess the degree of improvement obtained after the soil is treated. For soft soils, the rate of settlement after the treatment is over is considered to measure the effectiveness of the method. In this study, a load of 100 kPa was applied over the area to

observe the settlement of the ground surface before and after the treatment. It was observed that the settlements were reduced by 10 times after the treatment (Figure 4.16). A dimensionless parameter *Settlement Ratio* was introduced and for 300 days of load application period, its magnitude reduced from 0.15 at the beginning to 0.11 towards the end (Figure 4.17). Thus, the improvement in the soil properties was clearly highlighted in this study.
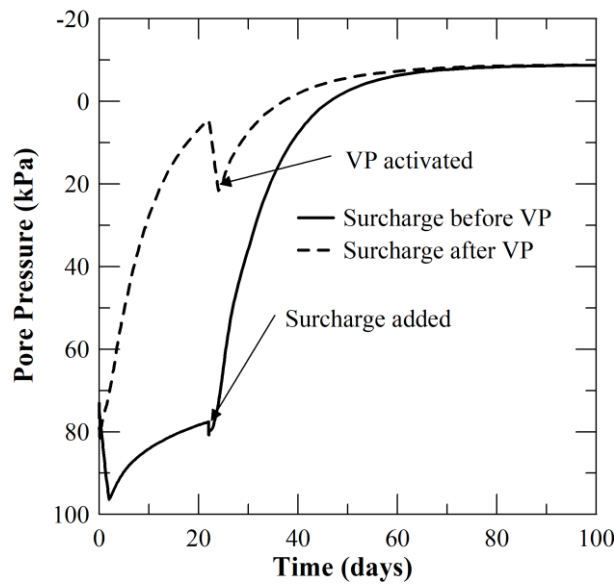
Figure 4.15: Comparison of Pore Pressure reduction when surcharge load is placed before and after the vacuum load is activated
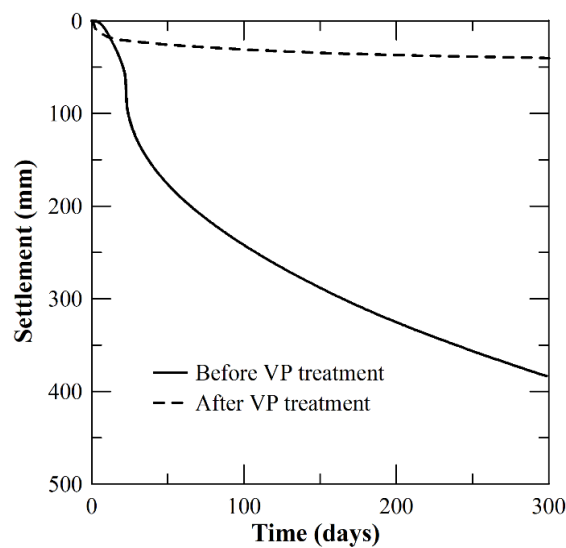
Figure 4.16: Comparison of Settlements before and after Vacuum Consolidation
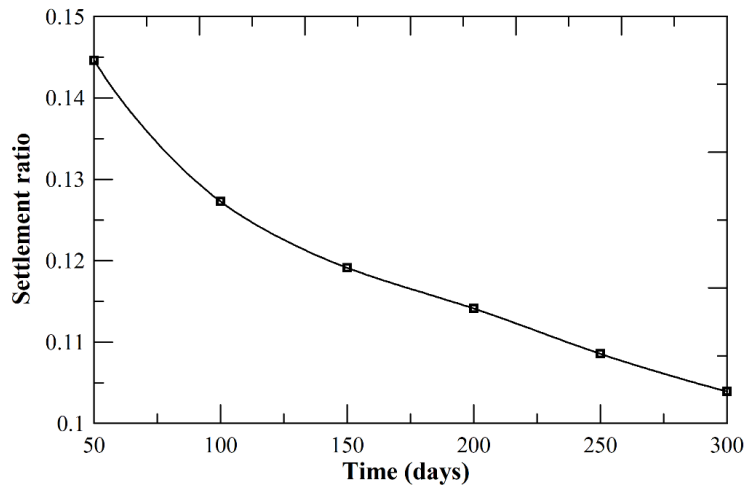
Figure 4.17: Decrease in ratio of settlements before and after the settlement with time

Influence of Poisson's ratio on Pore Pressure Reduction and Mandel Cryer effect

It was reported in section 4.4.2 that there is a temporary increase in the pore water pressure before it starts reducing, and this effect is termed as Mandel-Cryer effect. This phenomenon is commonly observed in surcharge or strip loads over the soil layer. However, it has been found to be very difficult to report this effect in field studies because of piezometer limitations. The pressure increase starts near the drainage boundary and then slowly transfers to the interior of the soil mass. This effect will not take place if the boundaries are impervious because the expulsion of water and the resulting volumetric stress generated due to squeezing of soil mass is a necessary condition. The magnitude of Mandel-Cryer effect also depends on Poisson's ratio (v'), as shown in Figure 4.18, it decreases with the increase in Poisson's ratio. The effect is almost negligible for $v' > 0.4$.
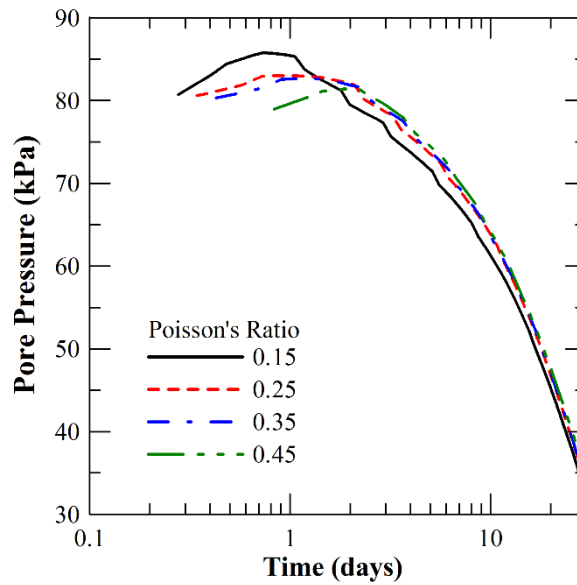
Figure 4.18: Influence of Poisson's ratio on pore pressure-time curve during Vacuum Consolidation

4.6 Summary

This study focused on the numerical analysis of the very first field trial of improvement of soft soil by vacuum consolidation method in India, at Kakinada, Andhra Pradesh. In 2D plane strain analysis, conversion of horizontal permeability as proposed by Indraratna et al. (2005) [20] was adopted so as to have same vacuum pressure throughout. Smear zone was not taken into consideration in this study. Settlements obtained from the numerical analysis were compared with the available field measurements and pore water pressure, lateral displacements, loss of vacuum pressure as predicted from the analysis were presented. A few parametric analyses were also conducted highlighting the influence of time of placement of surcharge load in surcharge assisted vacuum consolidation, influence of Poisson's ratio on pore pressure dissipation and Settlement characteristics of the soil before and after the improvement. The following conclusions can be drawn:

1. Convergence analysis was done to study the effect of closeness of model boundary to the treatment area. Thus, optimum width of model was established in the study. It was also found that the settlements did not depend on the element size of mesh. Coarse and fine mesh resulted in same settlement.

2. Numerical results are much higher than the field results. Difference in field and numerical results might be because of presence extra drainage paths in the soil strata. The vacuum applied through PVDs did not reach the soil layer completely.

3. Vacuum pressure loss in the field was predicted by modelling different cases. Maximum vacuum pressure developed in the field was estimated to be 30-35 kPa and in general 25-30 kPa.

4. Regions adjacent to drains show larger rate of drop in pore pressure when compared to the region between two drains. Points far from the drainage boundary show Mandel Cryer effect on vacuum pressure application. The magnitude of Mandel-Cryer effect was observed to be decreasing with increase in the Poisson's ratio.

5. DOC was calculated using the method suggested by Chu and Yan (2005) [4] considering pore pressure and was found to be in agreement with DOC obtained using settlement.

6. Inward lateral displacement was observed in soil mass at the perimeter of the treatment area. Maximum displacement was observed at the depth of 6m below the ground surface. Sand layer above the clay layer was found to restrict the inward movement at the surface, thus preventing surface cracks.

7. Staged vacuum application resulted in same settlement as that of single staged vacuum application. This advantage can be utilized while designing for long duration projects and may come up as an economic alternative when compared to single staged vacuum pressure application.

8. Application of surcharge load after the activation of vacuum load was found to be suitable to avoid sudden bearing failure when compared with surcharge load before the vacuum load.

9. Improvement in soil was evaluated with the settlement characteristics and the settlement was found to be reduced by 85-90 % after the treatment.

Chapter 5

Analysis of Radial Consolidation under Vacuum Preloading

5.1 Introduction

Vertical drains are installed to accelerate the consolidation process by introducing shorter, horizontal drainage paths. These horizontal drainage paths are essentially radial because of well nature of the drains. These vertical drains may be sand drains, perforated tubes or the PVDs. When surcharge will be applied over the ground surface, excess pore water pressure is generated in the soil. However, since the PVDs are always at atmospheric pressure, a head difference is created between the drain and the soil surrounding it. Thus, the water starts flowing from the soil into the drain and excess pore water pressure gets dissipated. In case of vacuum consolidation, the atmospheric pressure in the drain is replaced by a vacuum pressure, which discharges the water out of the soil mass.

5.2 Differential Equation for Radial Consolidation

Dissipation of excess pore water pressure in presence of a vertical drain is analyzed by considering a unit cell (Figure 5.1). A unit cell is basically a cylinder of radius equal to effective radius (r_e) of the vertical drain. The effective radius is the function of arrangement pattern of the drains, for triangular pattern, $r_e = 1.05*s$ whereas for square pattern, $r_e = 1.13*s$, where s is the center to center spacing between two adjacent drains.

To analyze a unit cell, the rectangular cross-section of the PVD must be first converted to an equivalent circular crow-section. This can be achieved by the following relation considering

the same perimeter of the converted cross-sectional area. The equivalent radius of the circular cross-section is given by:

$$r_w = \frac{(w+t)}{\pi}$$
(5.1)

Where w and t are the width and thickness of the PVD, respectively.
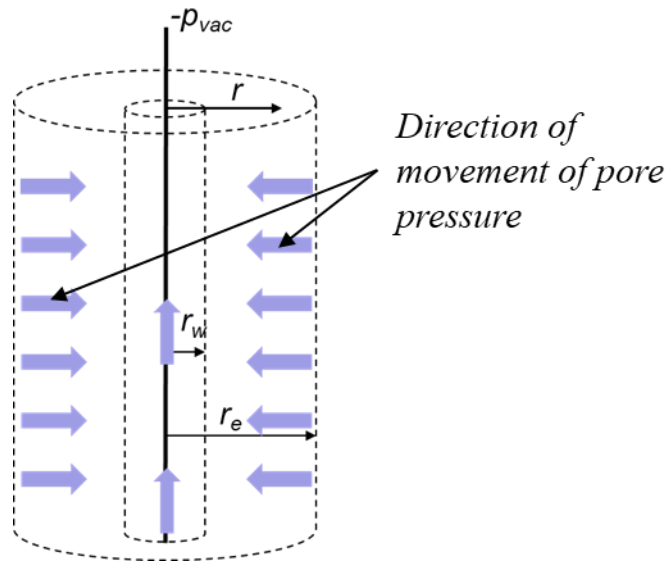
Figure 5.1: A vertical drain unit cell for problem of vacuum preloading

The differential equation governing the one-dimensional unsteady radial dissipation of pore pressure through a vertical drain is given as

$$\frac{\partial u}{\partial t} = C_r \left(\frac{\partial^2 u}{\partial r^2} + \frac{1}{r} \frac{\partial u}{\partial r} \right) \quad [7]$$
(5.2)

Where, t is the time elapsed after vacuum pressure application, r is the radial distance from the center line of the PVD, u is the excess pore pressure generated due to external load application and C_r is the coefficient of radial consolidation. In this equation $\frac{1}{r} \frac{\partial u}{\partial r}$ term takes care of the axisymmetric nature of the problem.

5.3 Nature of the Radial Consolidation Equation

The general form of the second order partial equation is given as

51

$$a\frac{d^2u}{dx^2} + b\frac{d^2u}{dxdy} + c\frac{d^2u}{dx} + d\frac{du}{dx} + e\frac{du}{dy} + fu = g(x, y) \qquad (5.3)$$

Where a, b, c, d, e and f are either constants or functions of only (x, y). These types of equations are called *linear equations*. Besides, if g(x, y) = 0, then the equation is said to be *homogenous*. For the above mentioned equation

if $b^2 - 4ac = 0$,   the equation is parabolic

if $b^2 - 4ac < 0$,   the equation is elliptic

if $b^2 - 4ac > 0$,   the equation is hyperbolic

From the above-mentioned conditions, the radial consolidation equation, $\frac{\partial u}{\partial t} = C_r\left(\frac{\partial^2 u}{\partial r^2} + \frac{1}{r}\frac{\partial u}{\partial r}\right)$ is parabolic in time and elliptical in space (radial line).

5.3.1   Boundary and Initial Conditions

The formulation of a problem requires complete specification of its geometry and appropriate boundary conditions. Besides, the equation is governed by a first derivative in time, so an initial condition is required in order to carry out the time integration. Whereas, the radial terms will require two boundary conditions, one each at the two boundaries of the domain. The boundary and initial conditions are stated as follows

$$u(r_w, t) = -p_{vac} \qquad (5.4a)$$

$$\frac{\partial u(r_e, t)}{\partial r} = 0 \qquad (5.4b)$$

$$u(r, 0) = 0 \qquad (5.4c)$$

In the boundary condition 4a, it is assumed that vacuum pressure $-p_{vac}$ is completely developed inside the well, i.e. up to the equivalent radius r_w of the drain.

5.4 Finite Difference Method

The finite difference method is one of the simplest and of the oldest methods to solve differential equations. The differential operator is approximated by replacing it with the difference quotients. The approximations are found using the space-time points which are

52

known as grid points. Problems are solved on a grid which has points uniformly spaced in each direction to ease the calculation and programming. The finite difference method works on the definition of derivative of a smooth function u at a point $x \in R$

$$u'(x) = \lim_{h \to 0} \frac{u(x+h) - u(x)}{h}$$ (5.5)

The parameter h should be sufficiently small to get a good approximation. The approximation is said to be 'good' when the error tends towards zero when h tends to zero. Error signifies the difference obtained in the value of the right-hand side in equation 2 when using derivative and difference quotient.

5.4.1 Difference quotients using Taylor series

If u_{i+1} is the excess pore pressure at a point $i+1$, then its Taylor series expansion about point i will be given by

$$u_{i+1} = u_i + \left(\frac{du}{dx}\right)_i \Delta x + \left(\frac{d^2 u}{dx^2}\right)_i \frac{(\Delta x)^2}{2} + \left(\frac{d^3 u}{dx^3}\right)_i \frac{(\Delta x)^3}{6} + \cdots$$ (5.6)

Considering Δx very small and thus neglecting the higher order terms in Δx, we obtain the following finite differences for first order derivatives

Forward difference $\qquad \left(\frac{du}{dx}\right)_i \approx \frac{u_{i+1} - u_i}{\Delta x}$ (5.7)

Backward difference $\qquad \left(\frac{du}{dx}\right)_i \approx \frac{u_i - u_{i-1}}{\Delta x}$ (5.8)

Central difference $\qquad \left(\frac{du}{dx}\right)_i \approx \frac{u_{i+1} - u_{i-1}}{2\Delta x}$ (5.9)

For second order derivatives

$$\frac{d^2 u}{dx^2} = \frac{1}{(\Delta x)^2}(u_{i+1} + u_{i-1} - 2u_i)$$ (5.10)

The graphical representation of the three finite difference schemes is demonstrated in Figure 5.2.
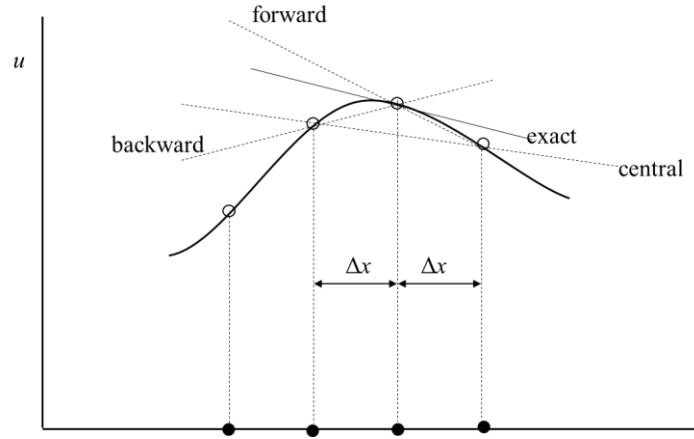
Figure 5.2: Forward, Backward and Central difference schemes for calculation of derivative

5.5 Formulation of Finite Difference

To formulate the finite difference scheme, we transform the terms u, t, and r to non-dimensional parameters $\bar{u}, \bar{t} \; and \; \bar{r}$ by the following relations

$$\bar{u} = \frac{u}{u_R} \tag{5.11}$$

$$\bar{t} = \frac{t}{t_R} \tag{5.12}$$

$$\bar{r} = \frac{r}{r_R} \tag{5.13}$$

Where u_R, t_R and r_R are reference pore pressure, reference time and reference radial distance respectively.

Using equations 2, 11, 12 and 13

$$\frac{1}{t_R}\frac{d\bar{u}}{dt} = \frac{C_r}{r_R^2}\left(\frac{dy}{dx} + \frac{1}{\bar{r}}\frac{dy}{dx}\right) \tag{5.14}$$

Choosing t_R in such a manner that $\frac{1}{t_R} = \frac{C_r}{r_R^2}$ and considering steps of Δr in radial direction and Δt (Δr and Δt being very small) for time, and assigning the normalized steps $\Delta \bar{r}$ and $\Delta \bar{t}$ (Figure 5.3) in the equations 7, 9 and 10, the equation 14 becomes

$$\frac{1}{\Delta \bar{t}}\left(\bar{u}_{r,\bar{t}+\Delta\bar{t}} - \bar{u}_{r,\bar{t}}\right) = \frac{1}{(\Delta\bar{r})^2}\left(\bar{u}_{r-\Delta\bar{r},\bar{t}} + \bar{u}_{r+\Delta\bar{r},\bar{t}} - 2\bar{u}_{r,\bar{t}}\right) + \frac{1}{\bar{r}}\left(\frac{\bar{u}_{r+\Delta\bar{r},\bar{t}}+\bar{u}_{r-\Delta\bar{r},\bar{t}}}{2\Delta\bar{r}}\right) \tag{5.15}$$

54

Further simplification results into

$$\bar{u}_{r,\bar{t}+\Delta\bar{t}} = \frac{\Delta\bar{t}}{(\Delta\bar{r})^2}\left\{\bar{u}_{r-\Delta\bar{r},\bar{t}} + \bar{u}_{r+\Delta\bar{r},\bar{t}} - 2\bar{u}_{r,\bar{t}} + \left(\frac{\bar{u}_{r+\Delta\bar{r},\bar{t}}+\bar{u}_{r-\Delta\bar{r},\bar{t}}}{2(\bar{r}/\Delta\bar{r})}\right)\right\} + \bar{u}_{r,\bar{t}} \qquad (5.16)$$

Equation 16 is the Finite difference scheme for calculating developed vacuum pressure at any point in the PVD unit cell under the influence of the vacuum pressure along the PVD.
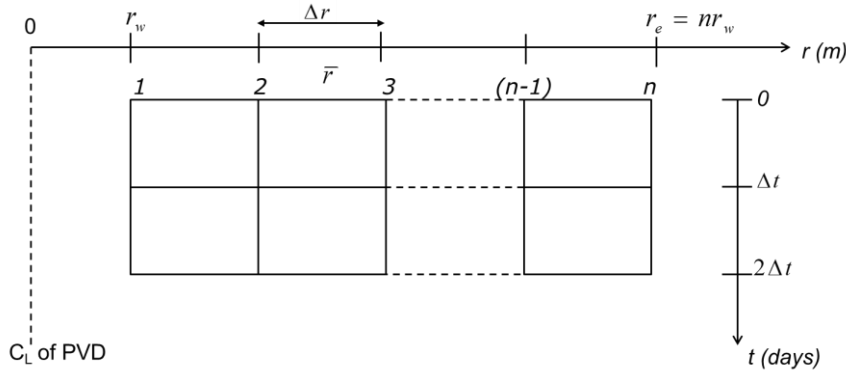

Figure 5.3: Finite difference discretization in (r, t) space

5.6 Algorithm

The effect of surcharge load was not considered in this analysis. Radial consolidation under only vacuum preloading was studied. Therefore, the initial excess pore pressure at any point in the unit cell outside the drain will be zero. The formulation for the algorithm was coded in MATLAB (vR2018a). The input parameters required to execute the program are: Coefficient of radial consolidation C_r, time period t, equivalent radius of the vertical drain r_w and the drain spacing ratio n. The algorithm followed to approach the solution is presented in Figure 5.4. After the declaration of the input parameters, reference parameters and time and radial steps are selected. Preferably, u_R and r_R are selected in such a way that $\bar{u}_i$ becomes 100, and $\bar{r}_e$ become n. This would ensure that the DOC is calculated directly form the pore pressure data. Besides, Δt should be chosen such that $\frac{\Delta\bar{t}}{(\Delta\bar{r})^2} < 0.5$. If this accuracy condition is not met, the program goes to the previous step and halves the time step Δt from the present value. This check is necessary to ensure that the time step is sufficiently small for the solution to converge.
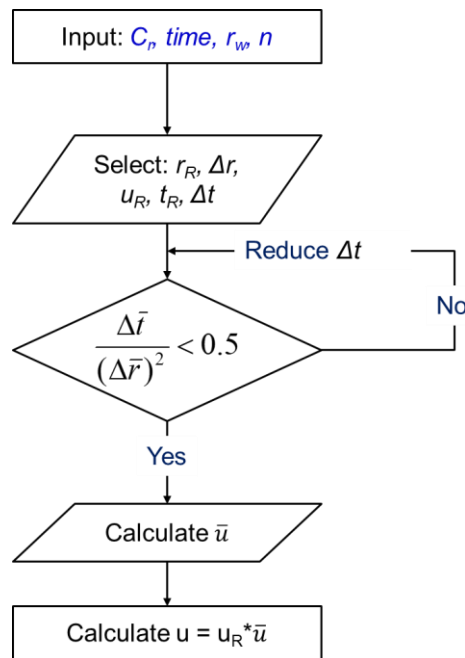
Figure 5.4: Algorithm for solving the equation

5.7 Results and Discussion

The program was executed for the following input parameters

$C_r = 0.0001$ to 0.01 m^2/day $n = 5$ to 25 and 100, $r_w = 0.033$ mm, time $= 10000$ days

The results of the program are presented in the form of DOC (U (%)) Vs. T_r (Radial Time Factor) plot. It was observed that for a lower value of n ($n = 5$), there was a difference of 5% DOC between $C_r = 0.0001$ m^2/day and $C_r = 0.01$ m^2/day. As n increases, the difference goes on diminishing and for $n \geq 15$, all the plots converge to a single line as seen in the Figures 5.5 - 5.9.
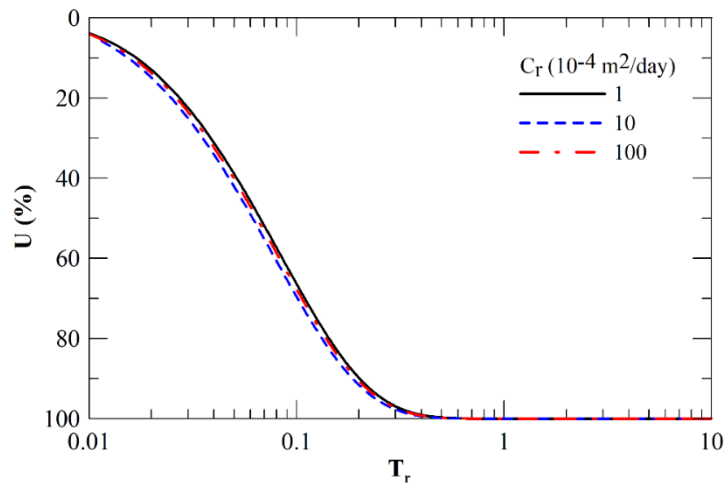
Figure 5.5: U vs T$_r$ plot for n = 5
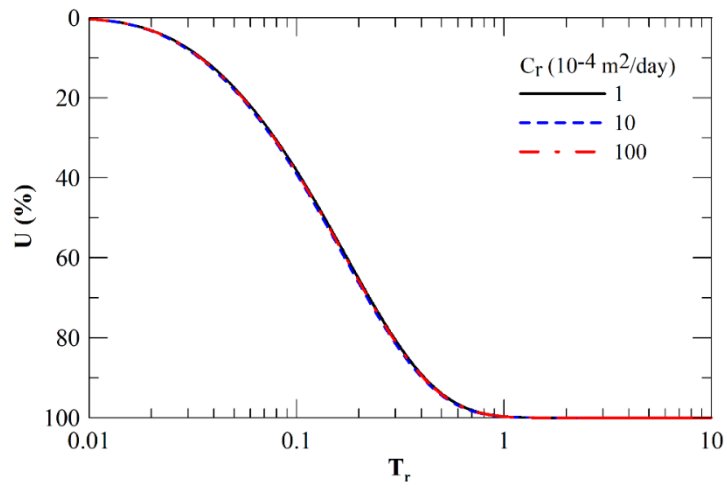
Figure 5.6: U vs T$_r$ plot for n = 10
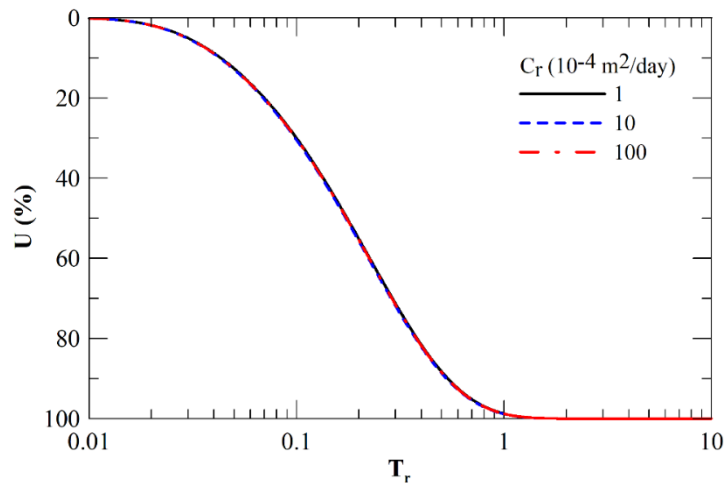
Figure 5.7: U vs. T_r plot for n = 15
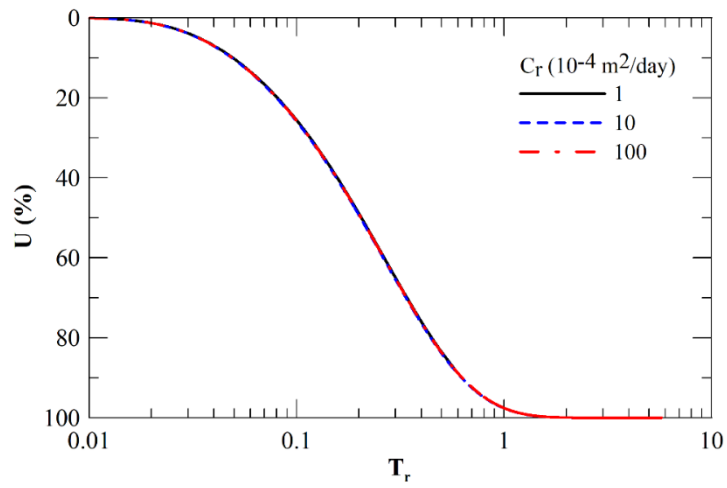
Figure 5.8: U vs. T_r plot for n = 20
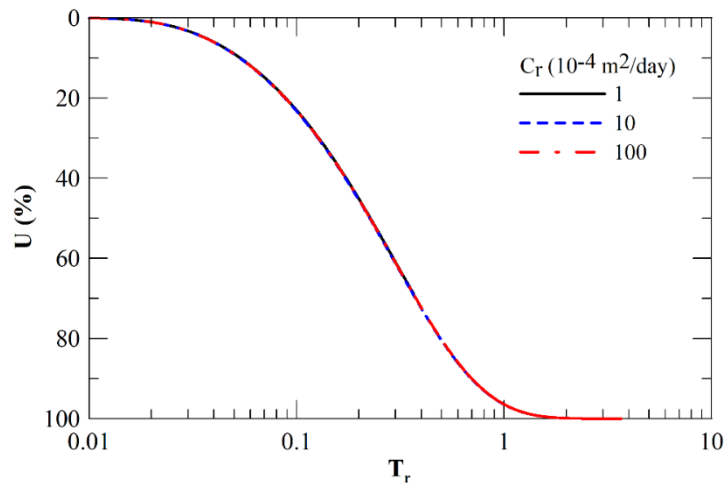
Figure 5.9: U vs. T_r plot for n = 25

5.8 Design Chart for Radial Consolidation under Vacuum Preload

The solutions for different *n* values can be clubbed together in a single plot and this will give us a design chart for the radial consolidation problem with vacuum preloading. It can be observed from Figure 5.10 that with increase in *n*, the *U* vs. T_r plots come closer to each other. Generally, *n* is kept in the range of 15 to 25 (spacing ~ 1 to 1.6 m) for ease in driving the PVDs. Higher *n* will cause longer time for achieving required DOC because of increased distance between drains.
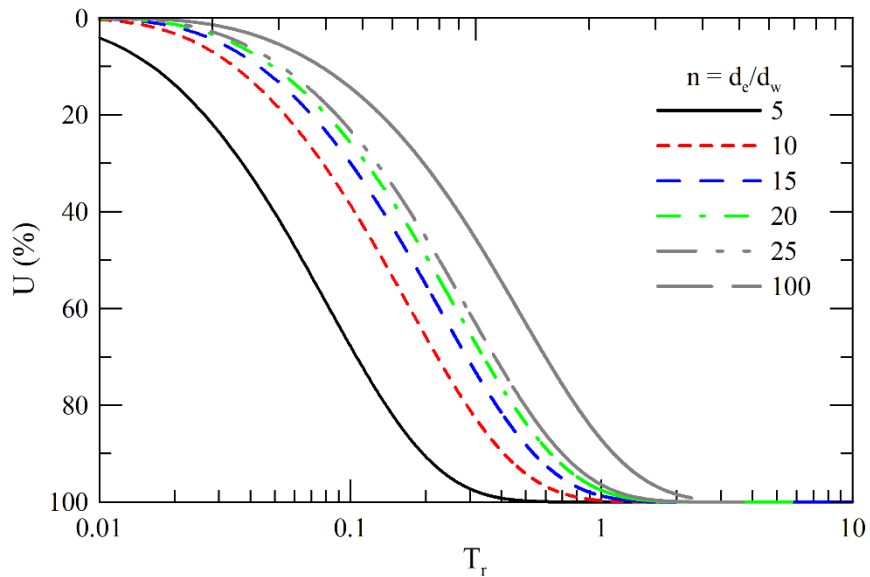
Figure 5.10: Generalized U vs T_r plot

The following steps are to be followed to find the time needed to achieve desired degree of consolidation.

1. Find the coefficient of radial consolidation (Cr) and the geometric parameters r_w, r_e and n

2. Fix the degree of consolidation required

3. Find T_r from the chart for desired U (%) for adopted n

4. Calculate time (t) using the expression $T_r = C_r \frac{t}{d_e^2}$

5.9 Application to case histories

Kakinada Port, India

The field study [27] at Kakinada port (Figure 4.1) was analyzed using the proposed chart. C_r was adopted as calculated using the available field observations. The adopted parameters are presented in the Table 5.1.

Table 5.1: Adopted properties for Kakinada port marine clay

C_r	0.012 m²/day
r_w	0.033 m
n	16 (calculated from drain

As per the measured field settlements, the DOC was calculated to be 70% in 28 days. From the chart (Figure 5.12), the DOC in 28 days was estimated to be 72%, which is close to the field observations.

Yaoqiang Airport Runway

Vacuum consolidation treatment was adopted for construction of runway at Yaoqiang airport, China [25]. The soft clay layer was found between the depths 7.5 m and 11.5 m. C_r was calculated using the measured settlement in the field after 90 days. The soil profile is as shown in Figure 5.10. The adopted properties are as summarized in Table 5.2.

3 m	Silty sand
2 m	Silty Clay
2.5 m	Silt
4 m	Soft Clay
8.5 m	Silty Clay
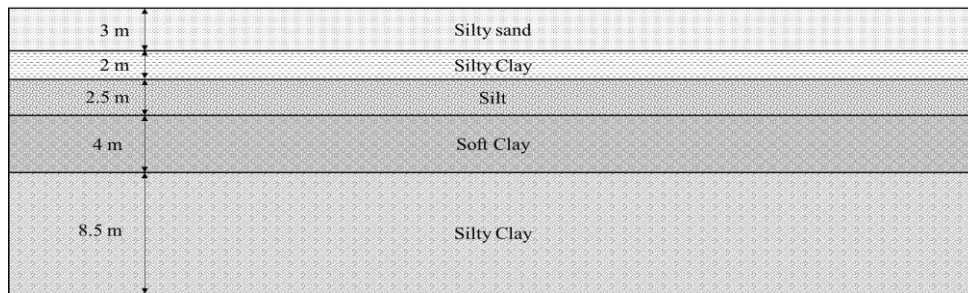
Figure 5.10: Soil profile at Yaoqiang airport site

Table 5.2: Adopted properties of soft clay soil from Yaoqiang Airport Runway, China

C_r	0.021 m²/day
r_w	0.033 m
n	25 (calculated from drain

From the field measurements, DOC was estimated to be 95%, from Figure 5.12, the DOC at 90 days was estimated to be 90% which differs from the field result by 5%, however, is sufficiently close.

Tianjin Port, China

Soil strata at Tianjin port was found to be in four layers [22], of which, the first and third layers were found to be similar and represented for the major depth of the soil; and hence, the properties corresponding to these layers were adopted for the rest of the layers as shown in Table 5.3. The soil profile is shown in Figure 5.11. For drain spacing of 1 m arranged in a square pattern, *n* was calculated to be 17. Settlements and pore pressures were recorded for 120 days.
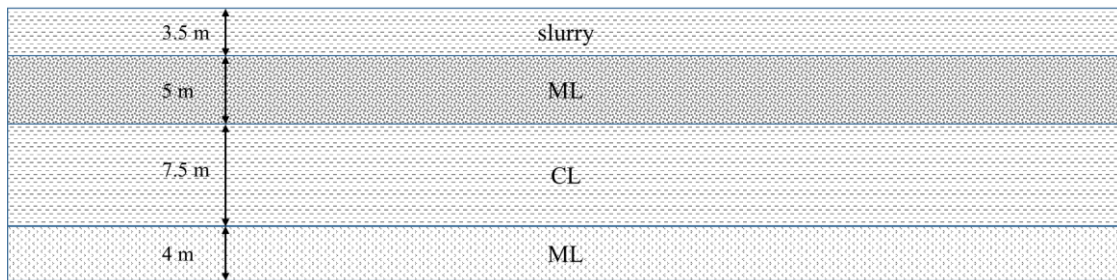
Figure 5.11: Soil profile at Tianjin port

Table 5.3: Adopted properties of soft clay soil from Tianjin port, China

C_r	0.0176 m²/day
r_w	0.031 m
n	17 (calculated from drain

DOC form field measurements were estimated to be 80% (using pore pressure profile as discussed in Section 4.4.2). DOC estimated using Figure 5.12 was slightly higher (~ 95 %) than the field results. The difference is possibly due to the layered soil stratification. This shows that the proposed design chart is not able to predict the behavior of layered soil closely. However, analysis of homogenous soil strata can be carried out with a fair degree of accuracy.
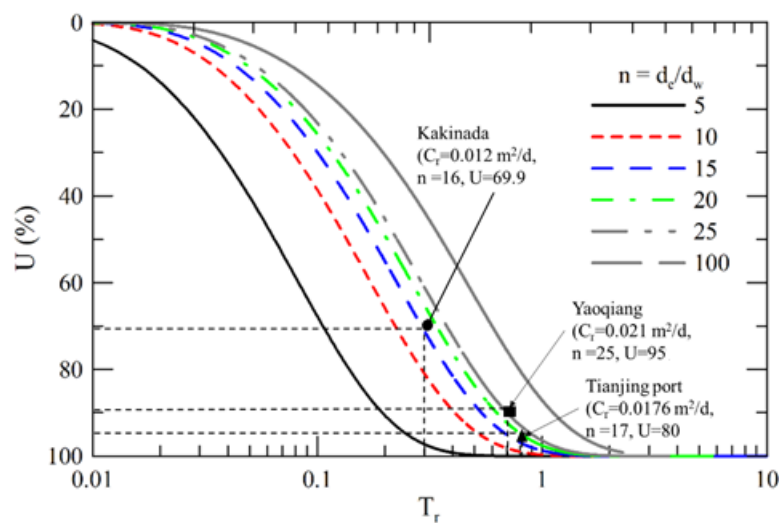
Figure 5.12: Application of Design Chart to Case Studies

5.10 Summary

This chapter describes the development of a finite difference formulation to solve the radial consolidation equation incorporating vacuum preload, without considering the effect of surcharge load. In this study, an individual vertical drain was analyzed using the unit cell approach. The nature of the radial consolidation equation was discussed and the influence of boundary conditions and initial conditions was described. The following conclusions were drawn from this part of the study:

1) The DOC achieved within a particular time is essentially a function of spacing of the PVDs.

2) For smaller value of n (n = 5), DOC achieved around $T_r=1.0$ was found be varying in a range of 5% for C_r values of 0.0001 m^2/day to 0.01 m^2/day. Thus, a band of lines was obtained for U vs. T_r plot.

3) As n increased, the band converged into a single line. Thus, with increased drain spacing, influence of C_r vanishes on the DOC.

4) The design chart obtained after solving the radial consolidation equation was in agreement with the homogenous soil strata, however the predictions for DOC were not accurate for a multi-layered soil system.

Chapter 6

Conclusions

6.1   General

In the present study, vacuum preloading method is modelled using PLAXIS 2D finite element software. Soft Soil model (based on Cam-Clay model) was considered to simulate the behavior of marine clay and linear drain elements are incorporated for PVDs. Vacuum pressure was simulated by reducing the groundwater head in the drains. The numerical model was validated with available case study at a port reclamation project in Vietnam and the results were found to be in good agreement with the published results. On the similar lines, a field study at Kakinada Port, India was modelled and the behavior of soft soil was analyzed under the influence of vacuum pressure. Parametric studies performed on the soft soil revealed that the change in pore water pressure depends on Poisson's ratio in the initial stage of vacuum pressure application. Further, a design chart was developed by solving the radial consolidation equation with vacuum preloading using Finite Difference method. The obtained plots were in good agreement with the homogenous single layered soils.

6.2   Conclusions

Study of Vacuum Consolidation in Kakinada Coastal Clay Deposits

Field study at Kakinada port was modelled and the influence of vacuum pressure on the behavior of soft soil was presented. The possible causes of loss of vacuum pressure during the field study were explored and the available vacuum pressure in the soil was predicted using numerical simulations. The following conclusions are drawn from the study:

1. Maximum vacuum pressure developed in the field was estimated to be 30-35 kPa and in general 25-30 kPa after simulating different cases for vacuum pressure loss.

2. Points far from the drainage boundary show Mandel Cryer effect on vacuum pressure application. The magnitude of Mandel-Cryer effect was observed to be decreasing with increase in the Poisson's ratio.

3. Sand layer above the clay layer was found to restrict the inward movement at the surface, thus preventing surface cracks.

4. Staged vacuum application resulted in same settlement as that of single staged vacuum application. This advantage can be utilized while designing for long duration projects and may come up as an economic alternative when compared to single staged vacuum pressure application.

5. Improvement in soil was evaluated with the settlement characteristics and the settlement was found to be reduced by 85-90 % after the treatment.

6.3 Analysis of Radial Consolidation under Vacuum Preloading

In this study, the radial consolidation equation was solved under the influence of vacuum pressure using the finite difference method. A wide range of parameters C_r (0.0001 to 0.01 m^2/day) and n (5 to 100) were considered. A design chart is proposed using the solutions obtained from solving the equation.

1. For smaller value of n (n = 5), and C_r values of 0.0001 m^2/day to 0.01 m^2/day, a band of curves was obtained for DOC vs. T_r plot instead of a single curve, thus indicating the influence of C_r on the DOC.

2. As n increased, the band converged into a single line. Thus, with increased drain spacing, influence of C_r vanishes on the DOC.

3. The design chart obtained after solving the radial consolidation equation was in good agreement with the homogenous soil stratum, however the predictions for DOC were not accurate for a multi-layered soil.

6.4 Scope of Future work

The present study focused on the behavior of soft soils under the influence of vacuum pressure. This study considered a homogenous soil stratum for the analysis. However, actual

soil profile may be non-homogenous or discontinuous which may pose additional challenges in the field. Presence of sand seams in the soil layer may be incorporated in future. Besides, since the area of treatment was kept small, the influence of surface area of the treatment can be analyzed. This study can be extended to the quantification of improvement in the behavior of soft soil after the treatment.

References

[1] G. Mesri, M.ASCE and A. Q. Khan, A.M.ASCE (2012) "Ground Improvement Using Vacuum Loading Together with Vertical Drains" J. Geotech. Geoenviron. Eng., 2012, 138(6): 680-689

[2] J.C. Chai, S. Hayashi and J.P. Carter (2005) "Characteristics of Vacuum Consolidation" Proceedings of the 16th International Conference on Soil Mechanics and Geotechnical Engineering, 1167-1170

[3] Cogon, J. M., Juran, I. and Thevanayakam, S. (1994) "Vacuum Consolidation Technology Principles and Field Experiences". Geotechnical Special Publication, No. 40, Vol. 2, ASCE, New York, pp.1237-1248.

[4] J. Chu and S. W. Yan (2005). "Estimation of Degree of Consolidation for Vacuum Preloading Projects." Int. J. Geomech., 2005, 5(2): 158-165

[5] Chu, J., and Yan, S.W. 2005. Application of vacuum preloading method in soil improvement project. Case Histories Book, Edited by Indraratna, B. and Chu, J., Elsevier, London. Vol. 3: 91-118

[6] Rujikiatkamjorn, C., Indraratna, B., and Chu, J. (2008). "2D and 3D numerical modeling of combined surcharge and vacuum preloading with vertical drains." Int. J. Geomech., 10.1061/(ASCE)1532-641(2008)8:2(144), 144–156.

[7] Barron, R. A. (1948). "The influence of drain wells on the consolidation of fine-grained soils." Dissertation, Providence, U.S. Eng. Office.

[8] Chai, Jun-Chun & Miura, Norihiko. (1999). Investigation of Factors Affecting Vertical Drain Behavior. Journal of Geotechnical and Geoenvironmental Engineering. 125. 10.1061/(ASCE)1090-0241(1999)125:3(216).

[9] Hansbo, S. (1981). Consolidation of Fine-grained Soils by Prefabricated Drains. Proceedings of the International Conference on Soil Mechanics and Foundation Engineering. 3. 677-682.

[10] Kjellman, W. (1952) "Consolidation of clayey soils by atmospheric pressure." Proc., Conf. on Soil Stabilization, Massachusetts Institute of Technology, Boston, 258–263.

[11] Indraratna, B., and Redana, I. W. (1998). Laboratory determination of smear zone due to vertical drain installation. J. Geotech. Eng., 125(1): 96-99.

[12] Sathananthan, I., Indraratna, B., and Rujikiatkamjorn, C. (2008). "Evaluation of smear zone extent surrounding mandrel driven vertical drains using the cavity expansion theory." Int. J. Geomech., 10.1061/(ASCE)1532-3641(2008)8:6(355), 355–365.

[13] Indraratna, B., Bamunawita, C., and Khabbaz, H. 2004. Numerical modeling of vacuum preloading and field applications. Canadian Geotechnical Journal. 41(6): 1098-1110.

[14] Robinson, Retnamony & Indraratna, B & Rujikiatkamjorn, Cholachat. (2012). Final state of soils under vacuum preloading. Canadian Geotechnical Journal. 49. 729-739. 10.1139/t2012-024.

[15] Chai, Jinchun & Carter, John & Hayashi, Shigenori. (2005). Ground Deformation Induced by Vacuum Consolidation. Journal of Geotechnical and Geoenvironmental Engineering - J GEOTECH GEOENVIRON ENG. 131. 10.1061/(ASCE)1090-0241(2005)131:12(1552).

[16] Mohamedelhassan, E. and J. Q. Shang (2002) Vacuum and Surcharge Combined One-Dimensional Consolidation of Clay Soils. Canadian Geotechnical Journal, 39(5), 1126-1138.

[17] Gangaputhiran S, Robinson RG and Karpurapu R (2016) Properties of soil after surcharge or vacuum preloading. Proceedings of the Institution of Civil Engineers – Ground Improvement 169(3): 217–230

[18] Biot, M. A. (1941) General Theory of Three-Dimensional Consolidation. Journal of Applied Physics, 12(2), 155-164.

[19] Hird, C. C., I. C. Pyrah and D. Russell (1992) Finite Element Modelling of Vertical Drains beneath Embankments on Soft Ground. Geotechnique, 42(3), 499-511.

[20] Indraratna, B., Sathananthan, I., Rujikiatkamjorn, C., and Balasubramaniam, A. S. (2005). "Analytical and numerical modelling of soft soil stabilized by PVD incorporating vacuum preloading." Int. J. Geomech., 5(2), 114–124

[21] Indraratna, B., and Redana, I. W. 2000. Numerical modeling of vertical drains with smear and well resistance installed in soft clay. Can. Geotech. J., 37(1): 132-145

[22] Cholachat Rujikiatkamjorn, Buddhima Indraratna, Jian Chu (2008) "2D and 3D Numerical Modeling of Combined Surcharge and Vacuum Preloading with Vertical Drains", International Journal of Geomechanics, Vol. 8, No. 2, April 1, 2008. ©ASCE, ISSN 1532-3641/2008/2-144–156

[23] Witasse, R., Racinais, J., Maucotel, F., Galavi, V., Brinkgreve, R., and Plomteux, C. (2012). Finite Element Modeling of Vacuum Consolidation using Drain Elements

and Unsaturated Soil Conditions. ISSMGE - TC 211 International Symposium on Ground Improvement IS-GI Brussels.

[24] Chu, J., S. W. Yan and H. Yang (2000) Soil Improvement by the Vacuum Preloading Method for an Oil Storage Station. Geotechnique, 50(6), 625-632.

[25] Tang, M. and J. Q. Shang (2000) Vacuum Preloading Consolidation of Yaoqiang Airport Runway. Geotechnique, 50(6), 613-623.

[26] Indraratna, B, Rujikiatkamjorn, C, Ameratunga, J & Boyle, P 2011, 'Performance and prediction of vacuum combined surcharge consolidation at Port of Brisbane', Journal of Geotechnical & Geoenvironmental Engineering, vol. 137, no. 11, 1009-1018.

[27] Shanmugam, Ganesh Kumar & Sridhar, G & Radhakrishnan, R & Robinson, Retnamony & Karpurapu, Rajagopal. (2014). A Case Study of Vacuum Consolidation of Soft Clay Deposit. Indian Geotechnical Journal. 45. 10.1007/s40098-014-0107-5.

[28] Abt, H. Land reclamation and soil improvement works for two deep water ports in Vietnam. Jpn. Geotech. Soc. Spec. Publ. 2016, 2, 1773–1777

[29] Wu, Hui & HU, Li-ming. (2013). Numerical model of soft ground improvement by vertical drain combined with vacuum preloading. Journal of Central South University. 20. 10.1007/s11771-013-1708-3.

[30] Indraratna, B., Kan, M. E., Potts, D., Rujikiatkamjorn, C. & Sloan, S. W. (2016). Analytical solution and numerical simulation of vacuum consolidation by vertical drains beneath circular embankments. Computers and Geotechnics, 80 83-96.

[31] Clough, R.W. & Woodward, R.J.. (1967). Analysis of embankment stresses and deformations. Journal of Soil Mechanics and Foundation Division. 93. 529-549.

[32] Reyes, S. F., and Deene, D. K. (1966). "Elastic Rustic Analysis of Underground Openings by the Finite Element Method," Proceedings of the 1st Congress of the International Society of Rock Mechanics, Lisbon, 477-486.

[33] Koteswara Rao D, Prasada Raju GVR (2011) Laboratory studies on the properties of stabilized Marine Clay from Kakinada Sea Coast, India. Int J Eng Sci Technol 3(1):421–428

[34] Tan, T. S., Inoue, T., and Lee, S. L. (1991). "Hyperbolic method for consolidation analysis." J. Geotech. Eng., 10.1061/(ASCE)0733-9410 (1991)117:11(1723), 1723–1737

[35] J. Mandel, Consolidation des Sols, G´eotechnique, 7, 287-299, 1953